(2)

Naval Research Laboratory

Washington, DC 20375-5000

NRL Memorandum Report 6228

Development of Sidebands in Tapered and in Untapered Free-Electron Lasers

B. HAFIZI

Science Applications International Corporation
McLean, VA 22102

A. TING

Berkeley Research Associates
Springfield, VA 22150

P. SPRANGLE AND C. M. TANG

Plasma Theory Branch
Plasma Physics Division

July 1, 1988

SECURITY CLASSIFICATION OF THIS PAGE

REPORT DOCUMENTATION PAGE

1a REPORT SECURITY CLASSIFICATION UNCLASSIFIED	1b RESTRICTIVE MARKINGS
2a SECURITY CLASSIFICATION AUTHORITY	3 DISTRIBUTION/AVAILABILITY OF REPORT Approved for public release; distribution unlimited.
2b DECLASSIFICATION/DOWNGRADING SCHEDULE	
4 PERFORMING ORGANIZATION REPORT NUMBER(S) NRL Memorandum Report 6228	5 MONITORING ORGANIZATION REPORT NUMBER(S)
6a NAME OF PERFORMING ORGANIZATION Naval Research Laboratory 6b OFFICE SYMBOL (If applicable) Code 4790	7a NAME OF MONITORING ORGANIZATION
6c ADDRESS (City, State, and ZIP Code) Washington, DC 20375-5000	7b ADDRESS (City, State, and ZIP Code)
8a NAME OF FUNDING/SPONSORING ORGANIZATION [illegible] 8b OFFICE SYMBOL (If applicable)	9 PROCUREMENT INSTRUMENT IDENTIFICATION NUMBER
8c ADDRESS (City, State, and ZIP Code) Washington, DC	10 SOURCE OF FUNDING NUMBERS PROGRAM ELEMENT NO 63221C; PROJECT NO W31RPD-7-D4039; TASK NO; WORK UNIT ACCESSION NO

11 TITLE (Include Security Classification)
Development of Sidebands in Tapered and in Untapered Free-Electron Lasers

12 PERSONAL AUTHOR(S)
Hafizi,* B., Ting,** A., Sprangle, P. and Tang, C.M.

13a TYPE OF REPORT	13b TIME COVERED	14 DATE OF REPORT (Year, Month, Day)	15 PAGE COUNT
Interim	FROM ____ TO ____	1988 July 1	51

16 SUPPLEMENTARY NOTATION
[illegible], Intl. Corp., McLean, VA 22102
[illegible] Assoc., Inc., Springfield, VA 22150

17 COSATI CODES		
FIELD	GROUP	SUB-GROUP

18 SUBJECT TERMS (Continue on reverse if necessary and identify by block number)
Free-electron laser; Tapered wiggler; Sideband frequencies; Nonadiabatic electron orbits

19 ABSTRACT (Continue on reverse if necessary and identify by block number)

A time-dependent, axisymmetric code is employed to examine the development of sidebands in a free-electron laser. For the case where the input signal undergoes an extended period of exponential growth, a broad spectrum of sidebands with growth rates comparable to that of the signal is excited. In general, in an untappered system the optical field displays considerable modulation after several synchrotron periods. An analytical model, in qualitative agreement with a number of features of the simulations, is discussed. In a tapered system the amplitude of the sidebands approaches a quasi-steady level that is several orders of magnitude below that of the untapered case, and the output optical field displays only a slight modulation. The optimal rate of tapering employed, to maximize efficiency, leads to substantial reduction in the growth rate of sidebands. This result is discussed in connection with the nonadiabatic nature of particle motion in the tapered system.

20 DISTRIBUTION/AVAILABILITY OF ABSTRACT ☐ UNCLASSIFIED/UNLIMITED ☐ SAME AS RPT ☐ DTIC USERS	21 ABSTRACT SECURITY CLASSIFICATION UNCLASSIFIED
22a NAME OF RESPONSIBLE INDIVIDUAL	22b TELEPHONE (Include Area Code) (202) 767-3493 22c OFFICE SYMBOL Code 4790

DD FORM 1473, 84 MAR — 83 APR edition may be used until exhausted. All other editions are obsolete. — SECURITY CLASSIFICATION OF THIS PAGE

CONTENTS

DEVELOPMENT OF SIDEBANDS IN TAPERED AND IN UNTAPERED FREE-ELECTRON LASERS

I. Introduction

In a free-electron laser (FEL) the synchrotron oscillation of electrons trapped in the ponderomotive potential well may couple energy into sideband frequencies. The ensuing instability leads to the modulation of the output signal and, in consequence, to an increase in its spectral width.

The growth of sideband frequencies has been the subject of discussion in a number of papers.[1-7] In the work presented herein this process is examined by means of a time-dependent code in an assumed axisymmetric geometry. Both tapered and untapered wigglers are examined. Two regimes of sideband development are examined in detail. In one, the carrier amplitude is small and all frequencies within the linear gain spectrum develop independently. In the other, the initial amplitude of the carrier is large and hence coupled to the sideband modes via the synchrotron oscillation of the electrons. Simplified analytical models of sideband growth in the two regimes are presented as an aid to understanding the important features of the simulations.

It should be emphasized at the outset that the numerical work reported herein is intended to contrast the development of sidebands in untapered and in tapered FEL systems. In this connection, the important issue of sideband start-up from the noise spectrum appropriate to the electron beam and wiggler parameters employed is not addressed.

Manuscript approved February 16, 1988.

II. Numerical Model

This section presents the equations that form the basis for the investigation of the FEL interaction.

The electrons move under the influence of the ponderomotive force due to the beating of the wiggler field with the optical field. The computations are simplified by employing the Gaussian-Laguerre Source-Dependent Expansion (SDE) technique,[8,9] thereby minimizing the number of Laguerre polynomials required for an accurate description of the optical field.

The optical field is taken to be of the form

$$\underline{a}_r(r,z,t) = \frac{1}{2}\, a(r,z,t)\, \exp\left[i\left(\frac{\omega}{c} z - \omega t\right)\right]\underline{e}_x + \text{c.c.} \quad ,$$

where $\underline{A}_r = mc^2\underline{a}_r/|e|$ is the radiation vector potential, m is the rest-mass of an electron, $|e|$ is the magnitude of the electronic change, c is the speed of light in vacuo, ω *is the radian frequency, and* $\underline{e}_x$ *is the unit* vector along the x axis. The wiggler field is assumed to be plane-polarized, of amplitude B_w and period $2\pi/k_w$:

$$\underline{B}_w(z) = \frac{-i}{2}\, B_w \exp(ik_w z)\underline{e}_y + \text{c.c.} \quad ,$$

where transverse variations of the wiggler field are neglected, and $\underline{e}_y$ is the unit vector along the y axis. The equations of motion of the j-th electron, of energy $\gamma_j mc^2$, are then given by

$$\frac{d\gamma_j}{dt} = \frac{i\omega a_w f_B}{4\gamma_j} \sum_n a_n L_n\left(2r_j^2/r_s^2\right)\exp\left[i\psi_j - (1-i\alpha)\, r_j^2/r_s^2\right] + \text{c.c.} \ , \tag{1}$$

$$\frac{d\psi_j}{dt} = ck_w\left(1-\gamma_r^2/\gamma_j^2\right) \ , \tag{2}$$

where

$$\gamma_r^2 = \frac{1}{2}\left(\omega/ck_w\right)\left(1 + a_w^2/2\right) \tag{3}$$

defines the resonant (i.e., synchronous) relativistic factor, $a_w = |e|B_w/mc^2k_w$ is the normalized vector potential of the wiggler, r_j is the radial distance of the j-th electron, $\psi_j = (\omega/c + k_w)\, z_j - \omega t$ is the relative phase with z_j the axial location of the j-th electron, and $f_B = J_o(\xi) - J_1(\xi)$ is the usual difference of Bessel functions, with $\xi = (a_w/2)^2/(1+a_w^2/2)$. The results to be presented in this paper pertain to the case where only a_w is tapered and the period of the wiggler is taken to be constant.

Following Sprangle et al.,[8] the envelope of the radiation field is expanded as follows

$$a(r,z,t) = \sum_n a_n(z,t)\, L_n\left[2r^2/r_s^2\right] \exp\left[-(1-i\alpha)r^2/r_s^2\right] .$$

Here, $\alpha(z,t)$ is related to the curvature of the optical wavefronts, $r_s(z,t)$ is the spot size, and $L_n\,(2r^2/r_s^2)$ is the Laguerre polynomial of degree n. The method of SDE then permits a complete specification of the optical field by solving[8]

$$\left(\frac{\partial}{\partial t} + c\,\frac{\partial}{\partial z}\right) r_s = \frac{2c^2\alpha}{\omega r_s} - r_s c\, B_I \ , \tag{4}$$

$$\left(\frac{\partial}{\partial t} + c\,\frac{\partial}{\partial z}\right) \alpha = \frac{2c^2(1+\alpha^2)}{\omega r_s^2} + 2c\left(B_R - \alpha B_I\right) , \tag{5}$$

$$\left(\frac{\partial}{\partial t} + c\,\frac{\partial}{\partial z} + cA_n\right) a_n = inBca_{n-1} + i\,(n+1)\, B^* ca_{n+1} - icF_n \ , \tag{6}$$

where

$$F_n = \frac{-\nu}{N\omega c} \left(\frac{2c}{r_s}\right)^2 \sum_j \left(\frac{f_B a_w}{\gamma}\right)_j L_n \left(2r_j^2/r_s^2\right) \exp\left[-i\psi_j-(1+i\alpha)r_j^2/r_s^2\right] , \quad (7)$$

$$A_n = \frac{2ic}{\omega r_s^2} (2n + 1 - i\alpha) + i\,(2nB_R + B) ,$$

and

$$B = F_1/a_o ,$$

$$\equiv B_R + i\,B_I . \quad (8)$$

In Eq. (7) the sum on j runs over the electrons in a given ponderomotive bucket and N denotes the number of electrons initially therein, and $\nu = I_b/(mc^2 v_z/|e|)$ is the Budker parameter, where I_b is the electron beam current.

A detailed presentation of the SDE approach is given in Ref. 8. For orientation, however, it should be noted that in vacuo one has the well-known result: $r_s(z) = r_s(0)\,(1+z^2/z_R^2)^{1/2}$, $\alpha = z/z_R$ where $r_s(0)$ is the minimum spot size (at z = 0) and $z_R = (\omega/2c)\, r_s^2(o)$ is the Rayleigh range. These results follow from Eqs. (4) and (5) upon neglecting B, i.e., neglecting the electron beam.

Typically 10 optical modes (n = 0, ..., 9) are included in the computations. As noted in the Introduction, the question of the proper spectrum and noise level for the sidebands due to spontaneous emission is not considered herein (see Ref. 10). The seed for the sideband frequencies may be incorporated in several ways. As an example, the noise level may be estimated from the Larmor formula and spread uniformly but with random phase over the computational spectrum. Although there are fluctuations between runs with different initial random phases, the general trend of

sideband development is as described herein. Finally, in all the computations the initial electron distribution is taken to be monoenergetic, the radial profile of the electron beam is taken to be parabolic, and betatron motion is neglected.

III. Numerical Results

For definiteness the parameters for the computations presented herein correspond to those of the Paladin experiment at the Lawrence Livermore National Laboratory,[11] and are listed in Table I.

In the linear regime the maximum growth rate obtains at the resonance wavelength λ_{res} = 10.34 μm. In what follows, where appropriate, a wavelength λ will be denoted in terms of the relative shift $\delta \equiv (\lambda/\lambda_{res})-1$ from the resonant value. Note that the wavelength of the carrier is given by $2\pi c/\omega$. Spectra are obtained by performing a spatial Fourier series analysis of the optical field $a(r=o,z,t)$ along the mesh. The result, displayed in the figures as Fourier amplitude, is dimensionless.

a) Multi-frequency, small input power

Simulations of a pulse of radiation extending over many ponderomotive buckets permit the development of frequencies besides that of the input signal, and as electrons slip relative to the radiation pulse the sideband instability may develop.

Figure 1 shows the development of 3 spectral components of the optical field when the input signal is at 10.6 μm ($\delta = 2.51\times10^{-2}$) and 100 W. Of course there are many other spectral components besides those shown in Fig. 1; however, the curves shown do indicate the general trend in the development of the sideband frequencies. Note in particular that in the exponential regime the growth rate of the component at $\delta = 0.77\times10^{-2}$ exceeds that of the main signal. This result is discussed in Section IV.

b) Multi frequency, untapered magnet

Figure 2 shows the development of the carrier for the case where 800 MW of 10.6 μm radiation ($\delta = 2.51\times10^{-2}$) is injected into an untapered magnet. Again, there are many modes in the spectrum that grow along the length of the wiggler. The dashed curve in Fig. 2 indicates the maximum

amplitude, or the envelope, of the rest of spectrum as a function of z. Fig. 2 also shows in detail the evolution of one of the fastest growing modes, at $\delta = 5.71\times10^{-2}$, indicating the trend in the development of the instability. At the end of the wiggler (25 m) the amplitude of the sidebands is large enough to spatially modulate the optical field by about 30%. Figure 3, which shows the phase of the carrier along the wiggler, will be discussed in connection with the analytical model for the instability in Section IV. At the wiggler exit the electron beam distribution function has a clear multi-stream character as indicated in Fig. 4. The spectrum of the optical field at this point consists principally of the carrier with a group of Stokes and anti-Stokes modes on either side, Fig. 5. The approximately symmetrical form of the spectrum, which is a reflection of comparable growth rates for modes symmetrically disposed with respect to the carrier, is discussed in Section IV.

c) Multi-frequency, tapered magnet

As is well known, for practical purposes the magnet employed in an FEL device must be tapered so as to enhance its efficiency and extraction. Figure 6 shows the development of the carrier and of the maximum amplitude of all the sidebands through a device where the normalized vector potential $a_w = |e|B_w/mc^2k_w$ is tapered as shown in Fig. 7. The form of the tapering employed in the computations is obtained by simply prescribing a constant rate of decrease of energy for a synchronous electron, at an assigned radius. From Eq. (3) with $d\gamma_r/dz$ = constant, one obtains $a_w(z)$. Comparing Figs. 2 and 6 it is apparent that in the tapered device the sidebands saturate at a level substantially below that of the carrier. As expected, the optical field is observed to be only slightly modulated in space. The electron distribution function (not shown here) consists principally of two

groups, an untrapped group and a trapped group at lower energy. Finally, Fig. 7 also shows the efficiency of the FEL, with 16% being a ten-fold improvement over the peak efficiency for the untapered device.

IV. Analysis of Results

An understanding of Fig. 1 may be obtained by performing a single-bucket linear stability analysis of Eqs. (1)-(7). The presentation is limited to the fundamental optical mode, and a monochromatic electron beam of energy $\gamma_o mc^2$ per electron.

Defining

$$\dot{\psi}_o = ck_w\,(1 - \gamma_r^2/\gamma_o^2),$$

$$\tilde{\psi}_j = \psi_j - \dot{\psi}_o t,$$

$$\Gamma_j = \gamma_j/\gamma_o,$$

$$A = ia\,\exp\,(i\dot{\psi}_o t),$$

the equilibrium corresponds to $A = 0$, $\Gamma_j = 1$, $\sum_j \exp(-in\tilde{\psi}_j) = 0$ $(n = 1, 2, \ldots)$.

Perturbing Eqs. (1)-(7), defining collective variables as in Ref. 12, and assuming a temporal dependence of the form exp $(-i\Upsilon t)$, the following dispersion relation is obtained

$$\Upsilon^3 + \left[\dot{\psi}_o - 2c^2(1-i\alpha)/\omega r_s^2\right]\Upsilon^2$$

$$+ \frac{\nu\left(a_w f_B\right)^2}{N\gamma_o^3}\left(\frac{c}{r_s}\right)^2 \sigma\,\Upsilon - 2\,ck_w\left(\frac{\gamma_r}{\gamma_o}\right)^2 \frac{\nu\left(a_w f_B\right)^2}{N\gamma_o^3}\left(\frac{c}{r_s}\right)^2 \sigma = 0\,,$$

where $\sigma = 2\sum_j (1 - r_j^2/r_s^2)\,\exp\,(-2\,r_j^2/r_s^2)$. Perturbing B [defined by Eq. (8)], and numerically solving Eqs. (4) and (5) along with the cubic in Υ, one obtains the growth rate, efficiency, spot size, and α in the exponential regime for any given angular frequency ω.

Now, as is well-known the FEL interaction has the rather important property that the optical field tends to be guided by the electron beam. In an amplifier operating in the exponential regime, it is found that,

irrespective of the initial spot size, the radiation beam asymptotes to a unique spot size r_s and wavefront curvature ($\sim \alpha^{-1}$) (Refs. 8 and 9). Figure 8 shows the growth rate Γ, efficiency η, matched spot size r_s and matched α in the case of a small input power as a function of $\delta = (\lambda/\lambda_{res})-1$, where $\lambda = 2\pi c/\omega$. The crosses are the results of single-bucket simulations. The curves are obtained from the linear stability analysis of the preceeding paragraph. It is seen that the agreement is quite good.

An important feature of Fig. 1 may now be understood with reference to Fig. 8. In the small signal regime - and therefore prior to particle trapping - Eqs. (1) - (7) may be linearized to show that there is no coupling between the various spectral components. In other words, the development of the spectral components proceeds independently and at a rate approximately equal to that indicated in Fig. 8. Referring to Fig. 1, it is thus seen that the larger growth rate of the sideband at $\delta = 0.77\times10^{-2}$ as compared to the carrier at $\delta = 2.51\times10^{-2}$ is consistent with Fig. 8.

It is also possible to set up and analyze a simple model of the FEL interaction so as to obtain an understanding of the gross features of the sideband instability ensuing from the synchrotron oscillation of the electrons in a large-amplitude carrier wave.

Neglecting diffraction and considering the fundamental mode of the optical field only, writing $\gamma_j = \gamma_r + \Delta\gamma_j(t)$, $\psi_j = \psi_{jo} + \Delta\psi_j(t)$, $a = |a^{(o)}| \exp[i\phi^{(o)}]$, the equilibrium is described by

$$\psi_{jo} + \phi^{(o)} + \alpha r_j^2/r_s^2 = 2n_j\pi \quad , \text{ (n_j is an integer)}$$

$$\frac{d^2}{dt^2}\Delta\psi_j = -\Omega_j^2\,\Delta\psi_j \ , \tag{9}$$

$$|a^{(o)}| = \text{constant}.$$

$$\left(\frac{\partial}{\partial t} + c\,\frac{\partial}{\partial z}\right)\phi^{(o)} \simeq \frac{\nu}{N\omega|a^{(o)}|}\left(\frac{2c}{r_s}\right)^2 \sum_j \frac{f_B a_w}{\gamma_r}\,\varepsilon_j\ , \tag{10}$$

where the synchrotron frequency is given by

$$\Omega_j = \left[\frac{ck_w \omega a_w f_B}{\gamma_r^{\,2}}\,|a^{(o)}|\,\varepsilon_j\right]^{1/2}\ ,$$

$\varepsilon_j = \exp\,(-r_j^{\,2}/r_s^{\,2})$, and γ_r is defined by Eq. (3). Note that Eq. (10) describes a linear increase in the equilibrium phase. Inserting numerical values corresponding to the wiggler entrance, Eq. (10) yields a rate of increase that is about a factor of 4 greater than that observed in Fig. 3 (beyond 9 m). Due to diffraction, however, the spot size r_s increases along the wiggler. Thus, inserting an average value for r_s (between 9 m and 25 m) the rate obtained from Eq. (10) is within several tens of percent of the numerical value.

Next, perturbing the equilibrium state and assuming a dependence of the form $f^{(1)} \sim \exp\,[-i(\Delta\omega t - \Delta k\ z)]$ for the perturbation, one obtains the following dispersion relation (Appendix A)

$$1 = \frac{1}{\chi^2} + \frac{\left(2\beta ck_w/\Omega_B\right)^2}{(\chi-\zeta)^2} - \frac{\beta}{\chi(\chi-\zeta)}\ , \tag{11}$$

where

$$\chi = \Delta\omega\left(1 + a_w^{\,2}/2\right)/2\Omega_B\gamma_r^{\,2}\quad ,\ \zeta = c\Delta k\left(1 + a_w^{\,2}/2\right)/2\Omega_B\gamma_r^{\,2}$$

$$\beta = \frac{\omega a_w f_B}{2|a^{(o)}|\gamma_r^{\,5}}\left(\frac{1 + a_w^{\,2}/2}{k_w r_s}\right)^2\left(\sum_j \varepsilon_j/N\right)\ ,$$

and

$$\Omega_B{}^2 = \sum_j \Omega_j{}^2/N \ . \qquad (12)$$

The dispersion relation is obtained in the <u>diagonal</u> approximation, wherein terms of the form $f^{(1)}\ \Delta\psi_j$, $f^{(1)}\ \Delta\gamma_j$ are neglected. The dispersion relation in Eq. (11) is similar to that given in Ref. 6. The last term on the right-hand side of Eq. (11), which is due to terms proportional to $\gamma_j{}^{(1)}$ and was neglected in Ref. 6, increases the growth rate by about 10%. In reference to the electron distribution function shown in Fig. 4, it is interesting to note the similarity of Eq. (11) to the dispersion relation for a multi-stream system. Neglecting the third term on the right-hand side of Eq. (11), it is seen that - as discussed in Ref. 6 - the dispersion relation has a symmetrical form about the carrier ($\Delta k = 0$), with identical growth rate for ($-\Delta\omega$, $-\Delta k$) and ($\Delta\omega$, Δk). The spectrum in Fig. 5 is in approximate agreement with this general feature of Eq. (11).

Inserting numerical values into Eq. (11), one finds that the range of unstable modes encompasses that obtained in the simulations. The maximum growth rate obtained is about a factor of 5 larger than the average value observed for one of the fastest growing modes in the simulations [cf. Fig. 2]. That the growth rate deduced from Eq. (11) should exceed that observed in the simulations and the discrepancy in the rate of increase of the phase of the carrier are to be expected for two reasons. First, diffraction of the optical field [neglected in deriving Eq. (11)] is bound to reduce growth rates. Second, in the simulations the electrons are distributed throughout the ponderomotive bucket with synchrotron frequencies ranging from Ω_j down to zero, whereas the analysis leading to Eq. (11) assumes all electrons to bounce at the bottom of the ponderomotive wells, at the largest synchrotron frequency [cf. Eq. (9)].

Turning next to the case of the tapered magnet, the question arises as to why the growth rate of the sidebands is about a factor of 6 smaller than that in the untapered magnet. [cf. Figs. 2 and 6]. As is well-known, upon tapering, the electrons separate into roughly two groups. For the tapering employed, the decelerating group - which is responsible for stimulated emission - comprises 25-30% of the total number of electrons. However, the sideband growth rate for such a fraction of the number of electrons is still large compared to the observed value. There appears to be additional reasons for the small growth rate of the sidebands. In the context of a high-extraction FEL with a tapered magnet it is generally assumed that the change of parameters (a_w and/or k_w) is slow enough so that the action $I_j \equiv \int d\psi_j \, (\gamma_j - \gamma_r)$ is an adiabatic invariant.[1] For the case considered here, however, it turns out that $d\gamma_r/dt \approx \Omega_j(\gamma_j - \gamma_r)$, implying that the action I_j is not an invariant (Appendix B). Additionally, the γ_j of trapped electrons decrease more or less monotonically with time, modifying the "equilibrium" electron distribution on the same time scale as that of the synchrotron motion. Physically, as the radiation pulse slips relative to the electrons, it is modulated not only by the synchrotron motion but also by the temporal variation of γ_r. This has a detuning effect and renders the sidebands quasi-stable. Indeed, by increasing the rate of tapering and therefore the rate of variation of γ_r, the modulation of the optical pulse is reduced further, although the efficiency is also diminished due to increased particle detrapping.

Finally, it is important to remark that the tapering employed here leads to the same efficiency for a single-bucket, single-frequency case as for a many-bucket, multi-frequency case. In other words, for the given analytical form for $a_w(z)$, the optimal rate of tapering naturally leads to the observed reduction in the growth rate of sideband modes.

V. Conclusion

The work presented here contrasts the development of sideband frequencies in an untapered and in a tapered magnet. For the tapering employed, optimal operation (i.e., maximum efficiency) is achieved when the electrons trapped in the ponderomotive buckets are non-adiabatically decelerated, leading to substantial suppression of the sideband frequencies relative to the untapered system.

Acknowledgement

Discussions with Dr. W. P. Marable are gratefully acknowledged. This work was supported by SDIO and managed by SDC.

Appendix A: Multi-frequency linear stability analysis

In this appendix some of the details leading to the dispersion relation in Eq. (11) are presented.

Upon writing $\gamma_j = \gamma_r + \Delta\gamma_j + \gamma_j^{(1)}$, $\psi_j = \psi_{jo} + \Delta\psi_j + \psi_j^{(1)}$, $\phi = \phi^{(o)} + \phi^{(1)}$, $|a| = |a^{(o)}| + |a^{(1)}|$, and neglecting terms comprising products of the form $\Delta\gamma_j\ \psi_j^{(1)}$, $\Delta\psi_j\ \gamma_j^{(1)}$, etc., one obtains, at first order,

$$\left(\frac{\partial}{\partial t} + c\,\frac{\partial}{\partial z}\right) |a^{(1)}| \simeq \frac{\nu}{N\omega} \left(\frac{2c}{r_s}\right)^2 \sum_j \frac{f_B a_w}{\gamma_r}\, \varepsilon_j \left(\psi_j^{(1)} + \phi^{(1)}\right) ,$$

$$|a^{(o)}| \left(\frac{\partial}{\partial t} + c\,\frac{\partial}{\partial z}\right) \phi^{(1)} \simeq -\frac{\nu}{N\omega} \left(\frac{2c}{r_s}\right)^2 \sum_j \frac{f_B a_w}{\gamma_r}\, \varepsilon_j \left(\frac{|a^{(1)}|}{|a^{(o)}|} + \frac{\gamma_j^{(1)}}{\gamma_r}\right) , \quad \text{(A1)}$$

$$\frac{d}{dt}\,\gamma_j^{(1)} \simeq -\frac{\omega a_w f_B}{2\gamma_r}\, \varepsilon_j\, |a^{(o)}| \left(\psi_j^{(1)} + \phi^{(1)}\right) ,$$

$$\frac{d}{dt}\,\psi_j^{(1)} = 2\, ck_w\ \gamma_j^{(1)}/\gamma_r ,$$

Note that the term proportional to $\gamma_j^{(1)}$ on the right-hand side of Eq. (A1) was neglected in Ref. 6 where a similar analysis of sideband growth was presented.

Defining collective variables

$$x_k = \sum_j \varepsilon_j^k \psi_j^{(1)}/N,\quad y_k = \sum_k \varepsilon_j^k \gamma_j^{(1)}/N,\quad E_k = \sum_j \varepsilon_j^k/N ,$$

one obtains

$$\left(\frac{\partial}{\partial t} + c\,\frac{\partial}{\partial z}\right) |a^{(1)}| = \frac{\nu}{\omega} \left(\frac{2c}{r_s}\right)^2 \frac{f_B a_w}{\gamma_r} \left(x_1 + E_1 \phi^{(1)}\right) ,$$

$$|a^{(o)}| \left(\frac{\partial}{\partial t} + c\,\frac{\partial}{\partial z}\right) \phi^{(1)} = -\frac{\nu}{\omega} \left(\frac{2c}{r_s}\right)^2 \frac{f_B a_w}{\gamma_r} \left(\frac{y_1}{\gamma_r} + \frac{E_1 |a^{(1)}|}{|a^{(o)}|}\right) ,$$

$$\frac{d}{dt} X_1 = \frac{2ck_w}{\gamma_r} y_1 ,$$

$$\frac{d}{dt} y_1 = - \frac{\omega\, a_w f_B}{2\gamma_r} |a^{(o)}| \left(X_2 + E_2\, \phi^{(1)}\right) ,$$

$$\frac{d}{dt} X_2 = \frac{2ck_w}{\gamma_r} y_2 ,$$

etc.

This hierarchy may be truncated by assuming $X_2 = \Sigma\varepsilon_j X_1/N$, $E_2 = \Sigma\varepsilon_j E_1/N$, whence

$$\frac{d^2}{dt^2} X_1 = - \Omega_B^{\,2} \left(X_1 + E_1\, \phi^{(1)}\right) ,$$

$$\frac{d}{dt} y_1 = - \frac{\gamma_r \Omega_B^{\,2}}{2ck_w} \left(X_1 + E_1\, \phi^{(1)}\right) ,$$

where Ω_B is defined by Eq. (12).

Assuming perturbations of the form exp $[-i(\Delta\omega t - \Delta kz)]$, one obtains the dispersion relation in Eq. (11), where the third term on the right-hand side is due to the term proportional to $\gamma_j^{(1)}$ on the right-hand side of Eq. (A1).

Appendix B: Temporal variation of adiabatic invariant

In this appendix, the law of variation of the action variable for the tapered magnet is obtained.

For a synchronous particle, the energy and phase evolve according to

$$\frac{d}{dt}\,\gamma_r = -\frac{\omega\, a_w f_B}{2\gamma_r}\,|a|\,\varepsilon_r \sin\left(\psi_r + \phi + \alpha r_r^2/r_s^2\right) ,$$

$$\frac{d}{dt}\,\psi_r = 0 .$$

Defining $\gamma_j = \gamma_r + \delta\gamma_j$, $\psi_j = \psi_r + \delta\psi_j$, the Hamiltonian for small amplitude oscillations is

$$H = \frac{ck_w}{\gamma_r}\,\delta\gamma_j^2 + \frac{\omega\, a_w f_B |a|}{4\gamma_r}\,\varepsilon_r \cos\left(\psi_r + \phi + \alpha r_r^2/r_s^2\right)\delta\psi_j^2 .$$

Defining the synchrotron frequency of such a particle,

$$\Omega_{syn} = \left[ck_w\omega\, a_w f_B |a|\,\varepsilon_r \cos\left(\psi_r + \phi + \alpha r_r^2/r_s^2\right)\right]^{1/2}/\gamma_r ,$$

following Ref. 13, the action (I_j) angle (w_j) variables are found to evolve according to

$$\frac{d}{dt}\,I_j = -\frac{I_j}{\gamma_r}\,\frac{d\gamma_r}{dt}\cos 2w_j ,$$

$$\frac{d}{dt}\,w_j = \Omega_{syn} + \frac{1}{2\gamma_r}\,\frac{d\gamma_r}{dt}\sin 2w_j .$$

These formulae are valid for the length of the magnet lying between 6 m and 21 m where Ω_{syn} is found to be remarkably constant in the simulations. Thus the variation of γ_r is the only factor contributing to the breaking of the adiabatic invariant I_j. (Generalization of the formulae to include the variation of Ω_{syn} in the other sections of the magnet is straightforward.) The change in the action variable over a synchrotron period is then found to be given by

$$\frac{|\Delta I|}{I} \lesssim \pi \left(\frac{d\gamma_r/dt}{\gamma_r \Omega_{syn}}\right)^2 ,$$

$$\sim 10^{-3} .$$

It is important to notice that although this variation is relatively small, it is nevertheless much faster than the usual case for an adiabatic invariant where $\Delta I \to 0$ exponentially as $d\gamma_r/dt \to 0$.

References

1. N. M. Kroll, P. L. Morton and M. N. Rosenbluth, IEEE J. Quantum Electron. QE-17, 1436 (1981).

2. J. C. Goldstein and W. B. Colson, in Proceedings of the International Conference on Lasers (STS, McLean, VA, 1982), p. 218.

3. A. T. Lin, in Physics of Quantum Electronics, edited by S. F. Jacobs, G. T. Moore, H. S. Pillof, M. Sargent III, M. O. Scully and R. Spitzer (Addison-Wesley, Reading, MA, 1982), Vol. 9, p. 409.

4. R. A. Freedman and W. B. Colson, Opt. Commun. 52, 409 (1985).

5. D. C. Quimby, J. M. Slater and J. P. Wilcoxon, IEEE J. Quantum Electron. QE-21, 979 (1985).

6. R. C. Davidson and J. S. Wurtele, Phys. Fluids 30, 557 (1987).

7. S. Riyopoulos and C. M. Tang, Nucl. Instrum. Methods Phys. Res., Sect. A 259, 226 (1987).

8. P. Sprangle, A. Ting and C. M. Tang, Phys. Rev. Lett. 59, 202 (1987); and Phys. Rev. A 36, 2773 (1987).

9. B. Hafizi, P. Sprangle and A. Ting, Phys. Rev. A 36, 1739 (1987).

10. P. Sprangle, C. M. Tang and I. Bernstein, Phys. Rev. Lett. 50, 1775 (1983); and Phys. Rev. A 28, 2300 (1983).

11. T. J. Orzechowski, E. T. Scharlemann, B. Anderson, V. R. Neil, W. M. Fawley, D. Prosnitz, S. M. Yarema, D. B. Hopkins, A. C. Paul, A. M. Sessler and J. S. Wurtele, IEEE J. Quantum Electron. QE-21, 831 (1985).

12. R. Bonifacio, C. Pellegrini and L. M. Narducci, Opt. Commun. 50, 373 (1984).

13. L. D. Landau and E. M. Lifshitz, Mechanics (Pergamon, New York, 1976), Sect. 49.

Table I. Parameters of the Paladin Experiment

Electron Beam	
Current	2 kA
Energy	50 MeV
Radius	0.45 cm
Magnet	
Induction	2.3 kG
Period	8 cm
Length	25 m
Radiation Field	
Wavelength	10.6 μm
Initial Spot Size	0.36 cm

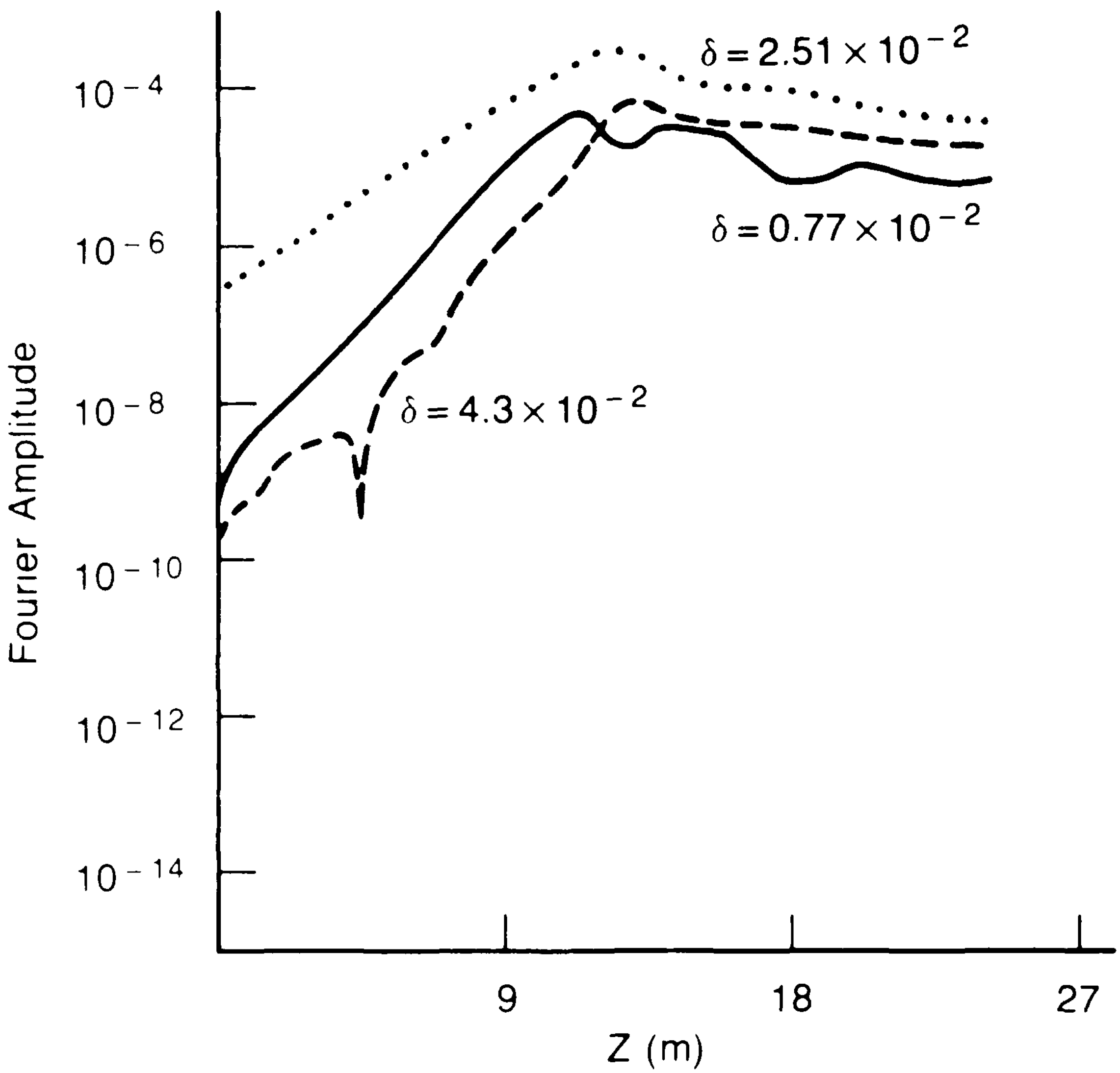

Fig. 1 Evolution of 3 spectral components along the wiggler when 100 W is input into the 10.6 μm wavelength ($\delta = 2.51 \times 10^{-2}$) at the entrance to the wiggler.

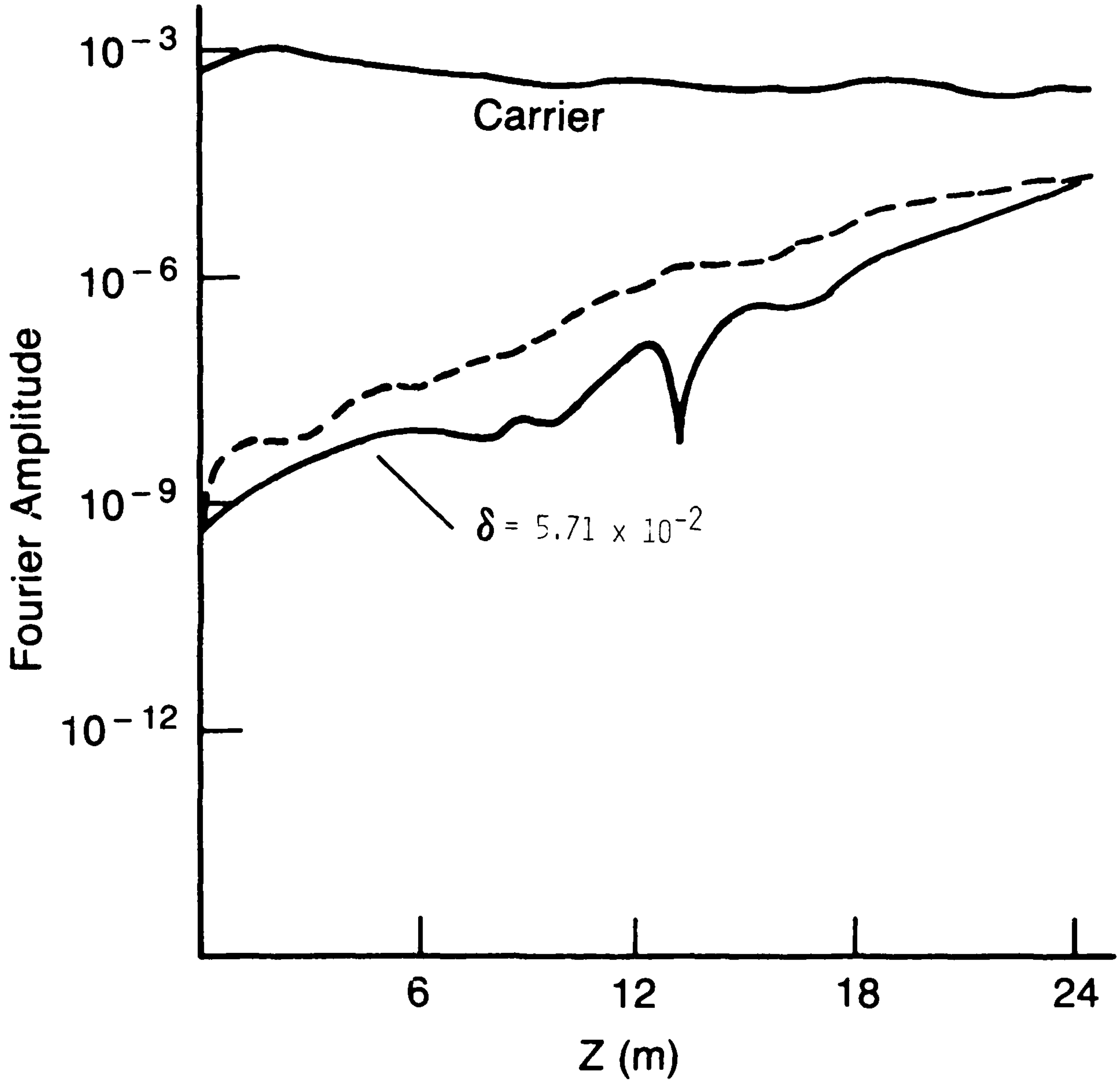

Fig. 2 Evolution of carrier (10.6 μm) starting from 800 MW in an untapered wiggler. The dashed curve indicates the upper bound for (or the envelope of) the rest of the spectrum. Also shown is the evolution of the sideband at $\delta = 5.71 \times 10^{-2}$ (10.93 μm).

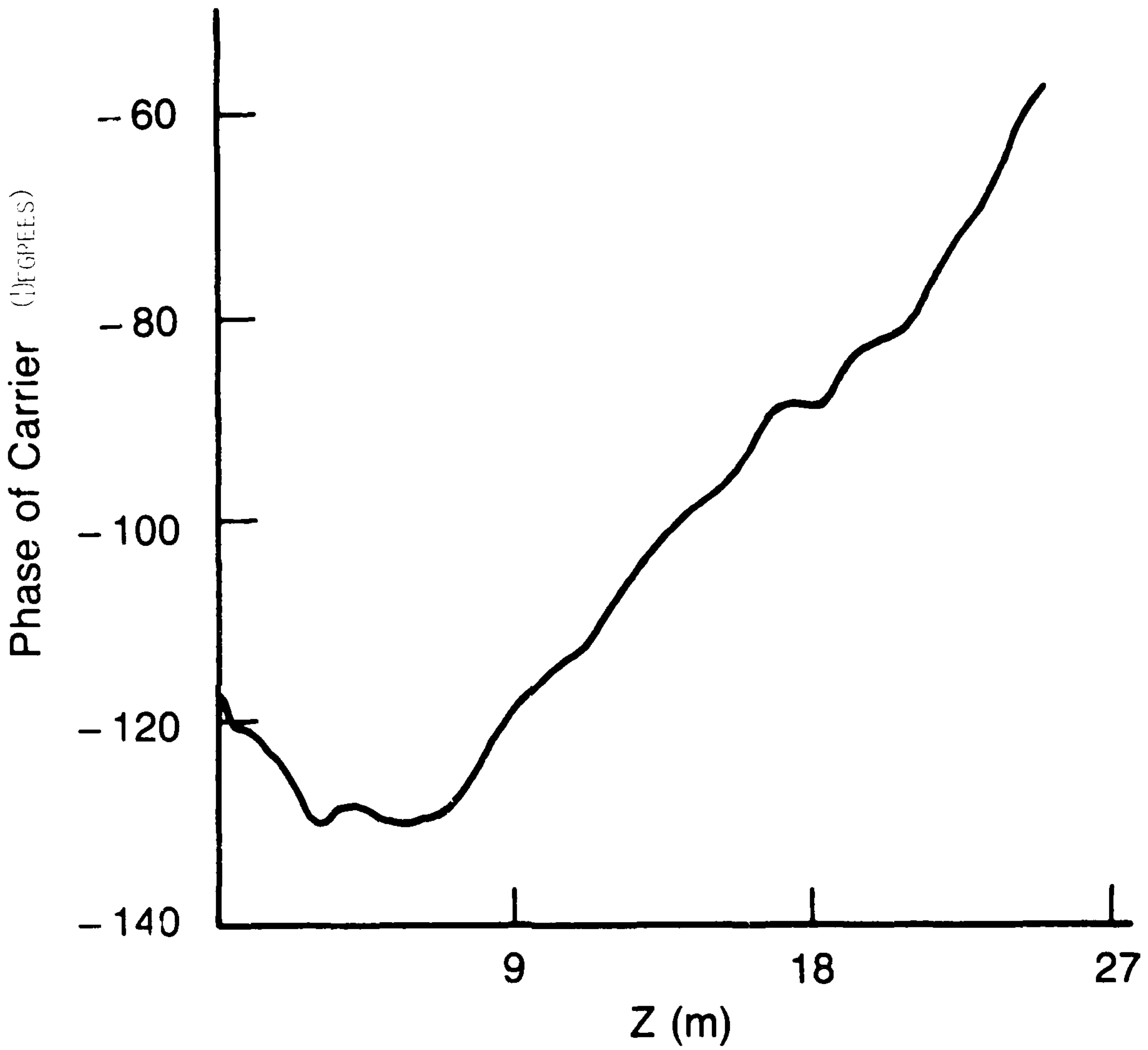

Fig. 3 Development of the phase of the carrier (in degrees) along the wiggler.

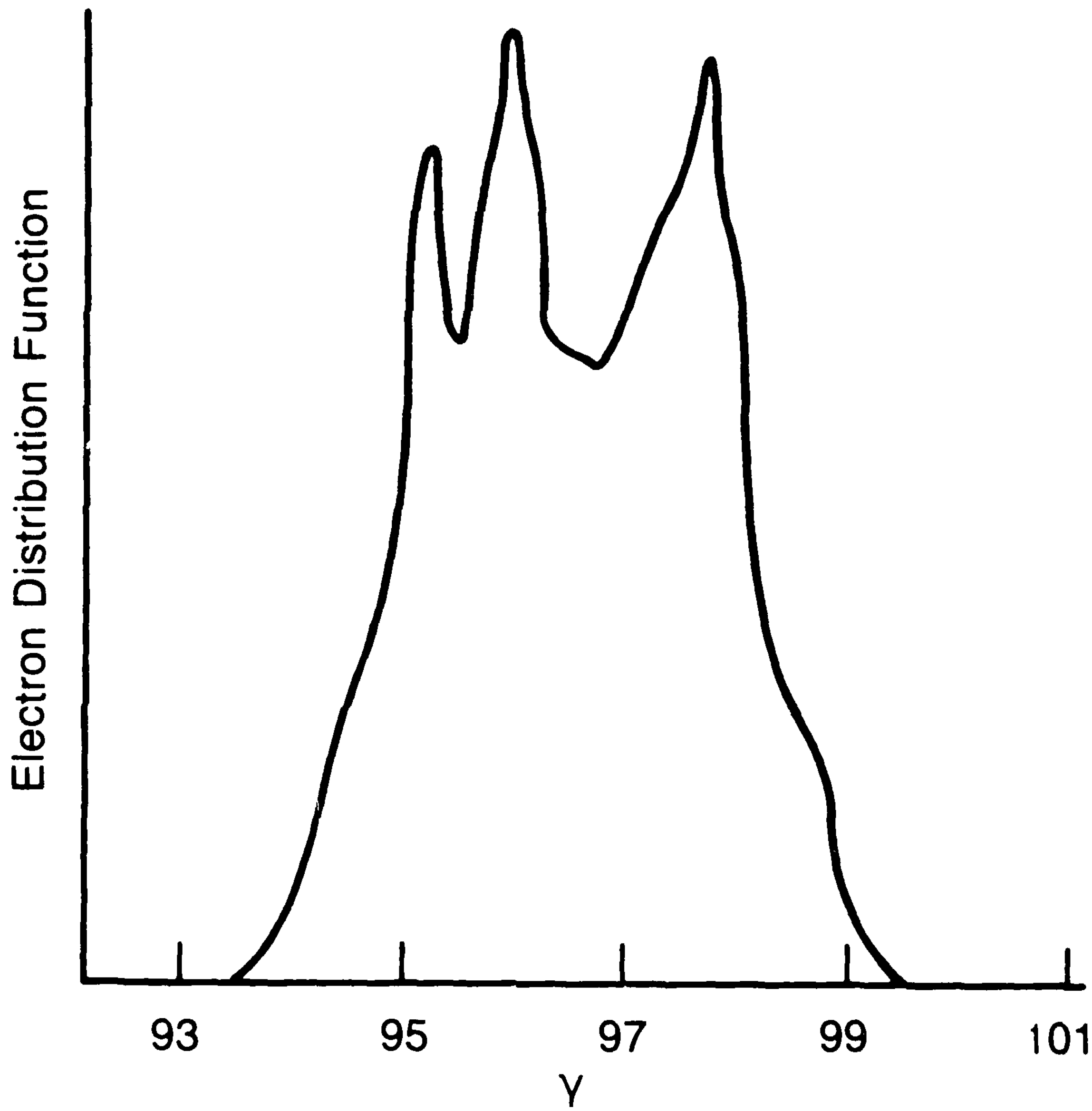

Fig. 4 Electron distribution function (i.e., number of electrons) versus relativistic mass factor γ at the end of the wiggler. (Ordinate scale is linear).

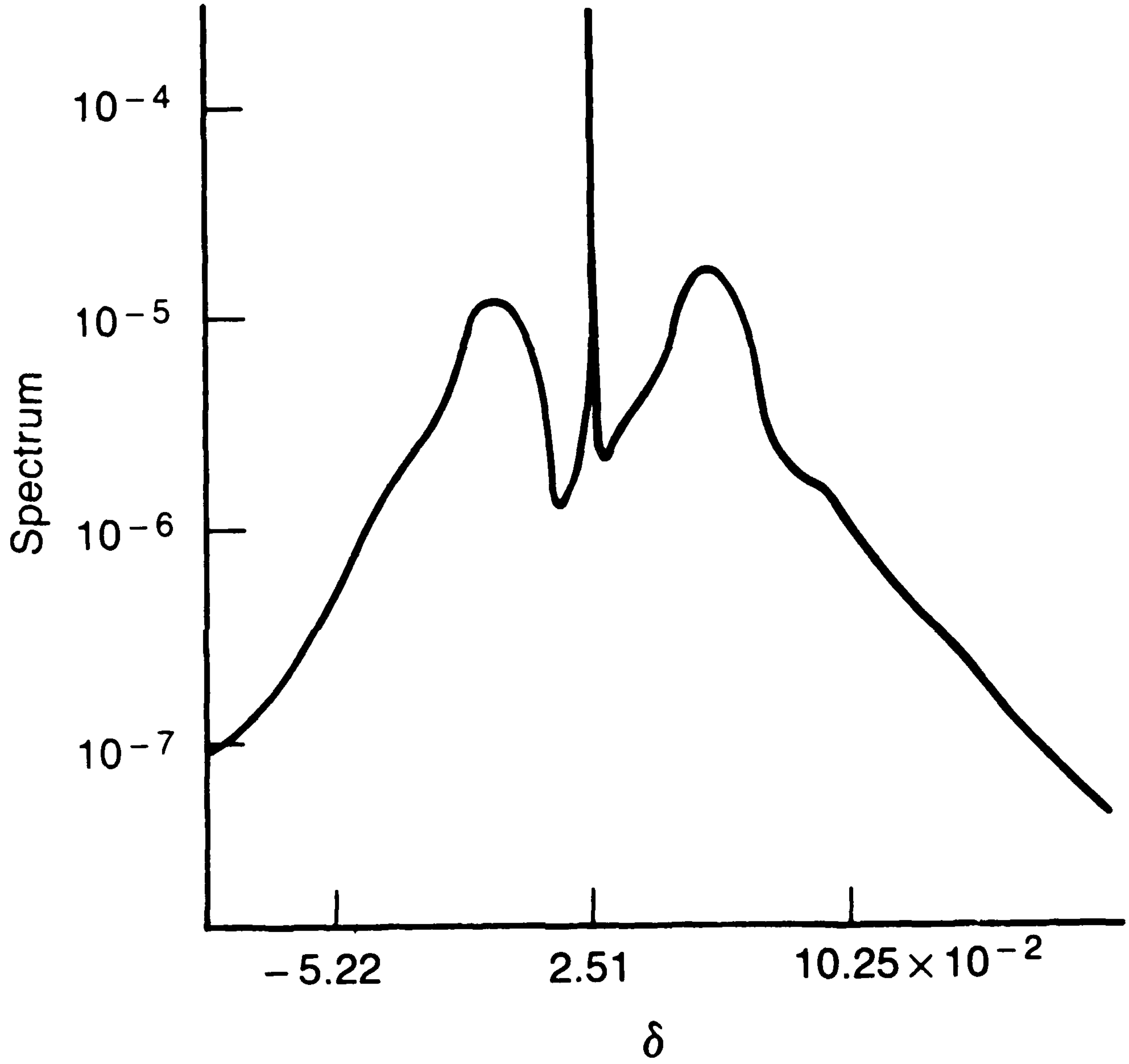

Fig. 5 Spectrum of optical field versus $\delta \equiv \lambda/\lambda_{res}-1$ at the end of the wiggler.

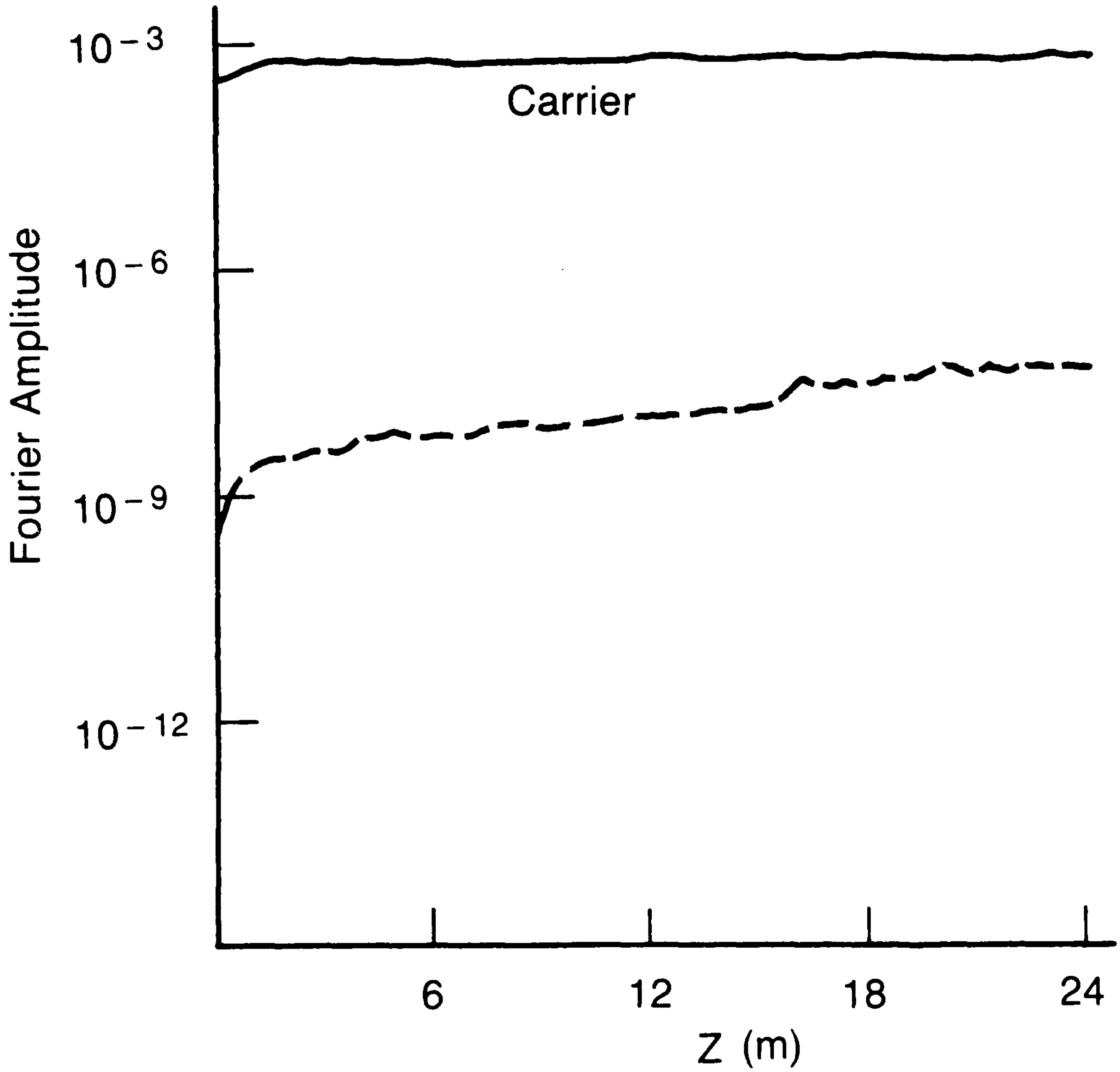

Fig. 6 Evolution of carrier (10.6 μm) starting from 800 MW in a tapered wiggler. The dashed curve indicates the upper bound for the rest of the spectrum.

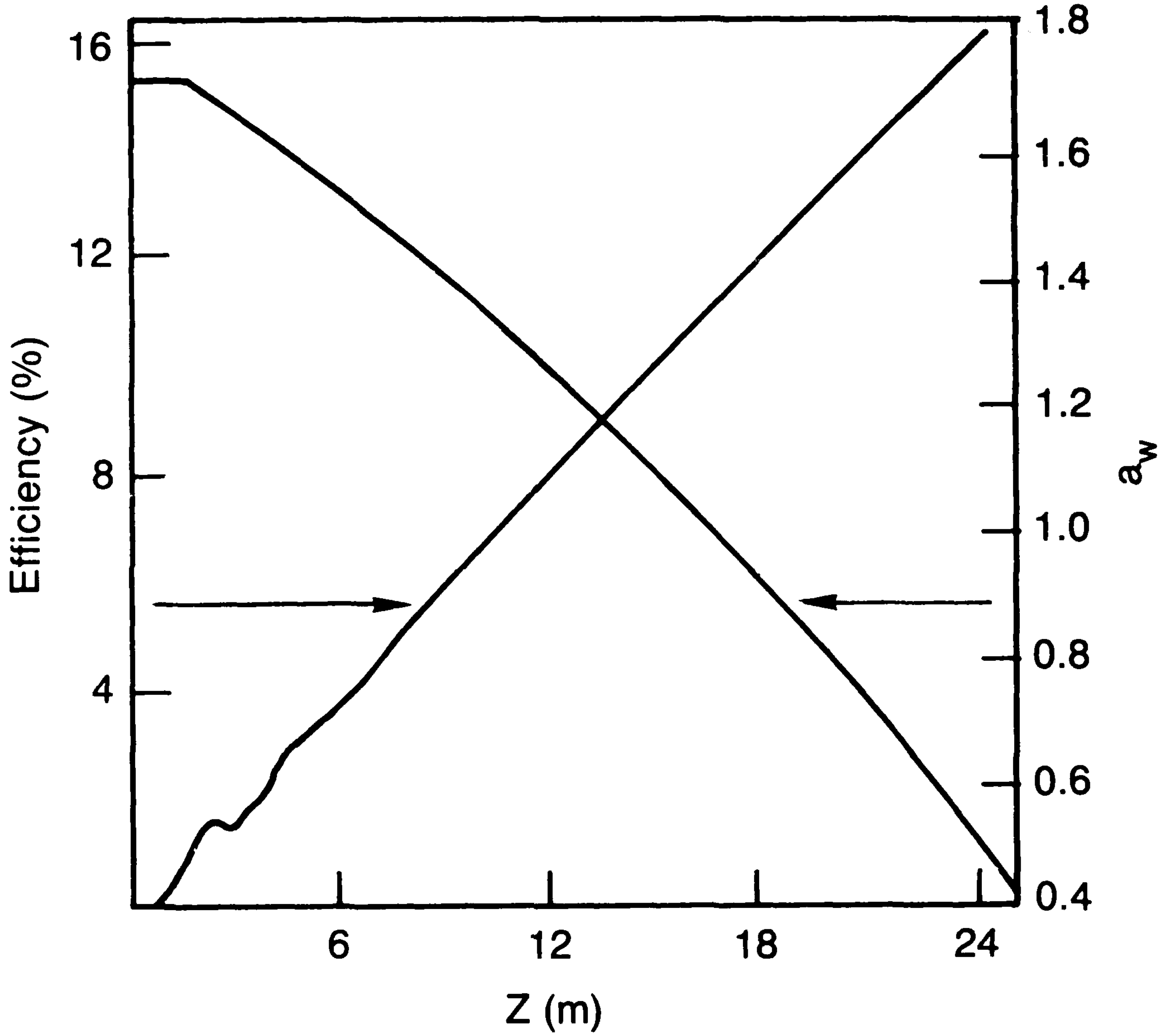

Fig. 7 Efficiency (%) and a_w along the length of the tapered magnet.

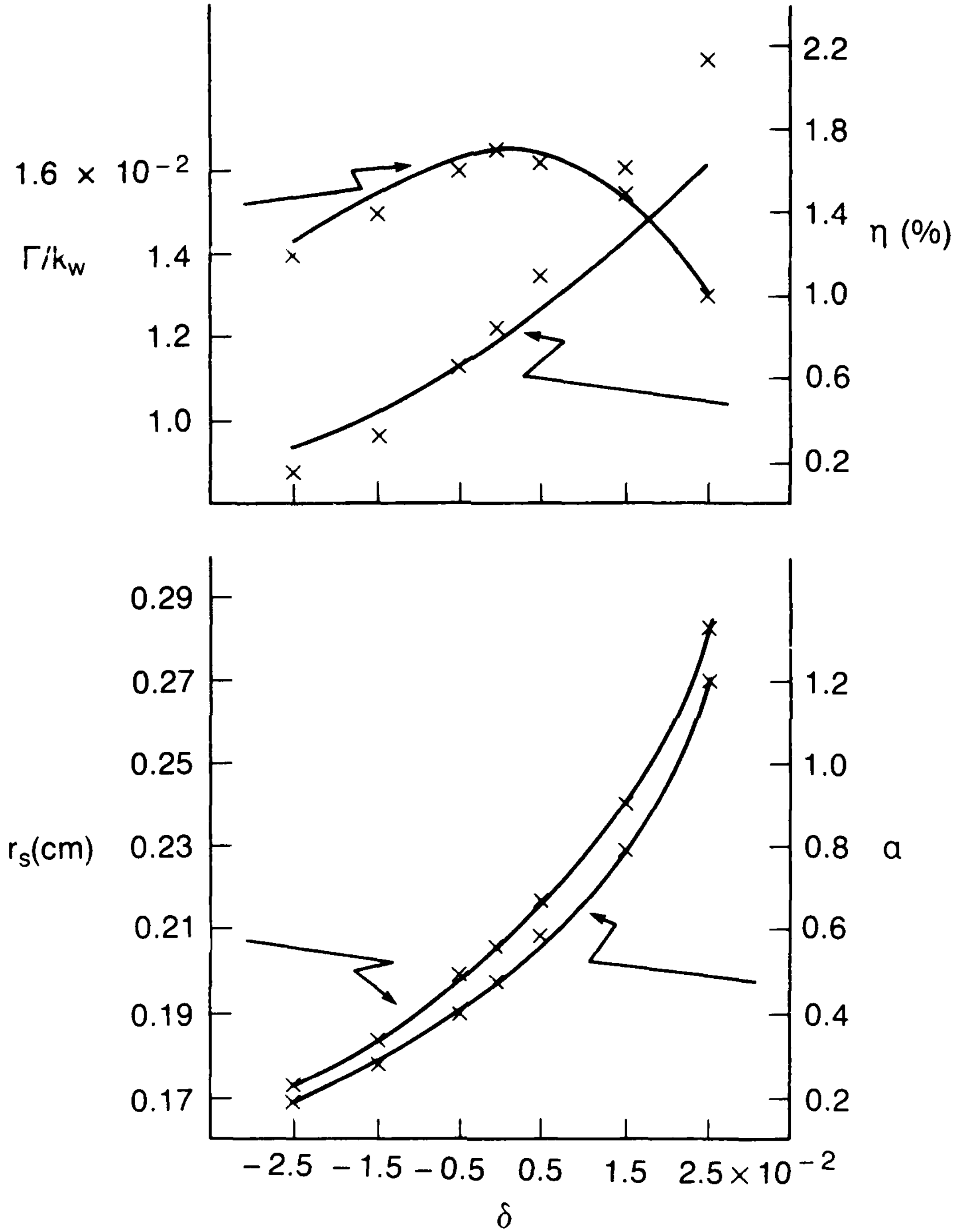

Fig. 8 Normalized growth rate Γ/k_w, efficiency $\eta(\%)$, spot size r_s, and α versus $\delta \equiv (\lambda/\lambda_{res})-1$, where $\lambda_{res} = 10.34$ μm. Crosses represent results of simulations. Curves are obtained from the linearized equations for the exponential, matched-optical-field regime. The electron beam radius is 0.3 cm.

DISTRIBUTION LIST*

Naval Research Laboratory
4555 Overlook Avenue, S.W.
Washington, DC 20375-5000

Attn: Code 1000 - Commanding Officer, CAPT W. G. Clautice
1001 - Dr. T. Coffey
1005 - Head, Office of Management & Admin.
1200 - CAPT M. A. Howard
1220 - Mr. M. Ferguson
2000 - Director of Technical Services
2604 - NRL Historian
4000 - Dr. W. R. Ellis
4600 - Dr. D. Nagel
4603 - Dr. W. W. Zachary
4700 - Dr. S. Ossakow (26 copies)
4700.1-Dr A. W. Ali
4710 - Dr. C. A. Kapetanakos
4730 - Dr. R. Elton
4740 - Dr. W. M. Manheimer
4740 - Dr. W. Black
4740 - Dr. J. Condon
4740 - Dr. A. W. Fliflet
4740 - Dr. S. Gold
4740 - Dr. D. L. Hardesty
4740 - Dr. A. K. Kinkead
4740 - Dr. M. Rhinewine
4770 - Dr. G. Cooperstein
4790 - Dr. P. Sprangle (50 copies)
4790 - Dr. C. M. Tang
4790 - Dr. M. Lampe
4790 - Dr. Y. Y. Lau
4790A- W. Brizzi
5700 - Dr. L. A. Cosby
6840 - Dr. S. Y. Ahn
6840 - Dr. A. Ganguly
6840 - Dr. R. K. Parker
6843 - Dr. R. H. Jackson
6843 - Dr. N. R. Vanderplaats
6875 - Dr. R. Wagner
2628 - Documents (20 copies)
2634 - D. Wilbanks

* Every name listed on distribution gets one copy except for those where extra copies are noted.

Dr. R. E. Aamodt
Science Appl. Intl. Corp.
1515 Walnut Street
Boulder, CO 80302

Dr. J. Adamski
Boeing Aerospace Company
P.O. Box 3999
Seattle, WA 98124

Dr. H. Agravante
TRW, Inc.
One Space Park
Redondo Beach, CA 90278 / R1-2020

Prof. I. Alexeff
University of Tennessee
Dept. of Electrical Engr.
Knoxville, TN 37916

Dr. L. Altgilbers
3805 Jamestown
Huntsville, AL 35810

Dr. A. Amir
Quantum Inst. and Dept. of Physics
University of California
Santa Barbara, CA 93106

Dr. Bruce Anderson
Air Force Weapons Laboratory
Kirtland AFB
Albuquerque, NM 87117

Dr. Antonio Anselmo
909 Mitchell Street
Cornell University
Ithaca, NY 14850

Dr. T. M. Antonsen
University of Maryland
College Park, MD 20742

Dr. C. M. Armstrong
Code 6843
Naval Research Laboratory
Washington, DC 20375-5000

Dr. Tony Armstrong
Science Applications Intl. Corp.
P.O. Box 2351
La Jolla, CA 92038

Assistant Secretary of the
Air Force (RD&L)
Room 4E856, The Pentagon
Washington, D.C. 20330

Dr. W. P. Ballard
Sandia National Laboratories
ORG. 1231, P.O. Box 5800
Albuquerque, NM 87185

Mr. Jon Barber
Dept. of Physics
Bethel College
St. Paul, MN 55112

Dr. W. A. Barletta
Lawrence Livermore National Lab.
P. O. Box 808
Livermore, CA 94550

Dr. L. R. Barnett
3053 Merrill Eng. Bldg.
University of Utah
Salt Lake City UT 84112

Commander George Bates, PMS 405-300
Naval Sea Systems Command
Department of the Navy
Washington, DC 20362

Dr. Latika Becker
U. S. Army SDC
DASD-H-F
P. O. Box 1500
Huntsville, AL 35807-3801

Dr. W. Becker
Univ. of New Mexico
Institute for Mod. Opt.
Albuquerque, NM 87131

Dr. Robert Behringer
Code 818
Office of Naval Research
1030 E. Green
Pasadena, CA 91106

Dr. G. Bekefi (5 copies)
Mass. Institute of Tech.
Bldg. 26
Cambridge, MA 02139

Dr. S. Bender
Los Alamos National Laboratory
P. O. Box 1663
Los Alamos, NM 87545

Dr. J. Benford
Physics International
2700 Merced Street
San Leandro, CA 94577

Dr. Herbert S. Bennett
National Bureau of Standards
Bldg. 225, Rm. A352
Washington, DC 20234

Dr. S. Benson
S.P.R.C.
Dept. of Physics
Stanford University
Stanford, CA 94305

Dr. T. Berlincourt
Office of Naval Research
Attn: Code 420
Arlington, VA 22217

Dr. I. B. Bernstein (10 copies)
Mason Laboratory
Yale University
400 Temple Street
New Haven, CT 06520

Dr. Vladislav Bevc
Synergy Research Institute
P.O. Box 561
San Ramon, CA 94583

Dr. Anup Bhowmik
Rockwell International/Rocketdyne Div.
6633 Canoga Avenue, FA-40
Canoga Park, CA 91304

Dr. K. Jim Bickford
RDA
2301F Yale Blvd., S.E.
Albuquerque, NM 87106

Dr. D. L. Birx
Lawrence Livermore National Laboratory
P. O. Box 808
Livermore, CA 94550

Dr. J. Bisognano
Lawrence Berkeley Laboratory
University of California, Berkeley
Berkeley, CA 94720

Dr. Steve Bitterly
Rockwell International/Rocketdyne Div.
6633 Canoga Avenue, FA-40
Canoga Park, CA 91304

Dr. H. Boehmer
TRW DSSG
One Space Park
Redondo Beach, CA 90278

Dr. P. Bosco
KMS Fusion Inc.
Ann Arbor, MI 48106

Dr. I. Boscolo
Quantum Institute
University of California
Santa Barbara, CA 93106

Dr. B. Boswell
Lab for Laser Energetics
University of Rochester
250 E. River Road
Rochester, NY 14623

Dr. G. Bourianoff
1901 Rutland Drive
Austin, TX 78758

Dr. J. K. Boyd
Lawrence Livermore National Laboratory
P. O. Box 808
Livermore, CA 94550

Dr. H. Brandt
Department of the Army
Harry Diamond Laboratory
2800 Powder Mill Rd.
Adelphi, MD 20783

Dr. Charles Brau (2 copies)
Los Alamos National Laboratory
P.O. Box 1663, M.S. - 817
Los Alamos, NM 87545

Dr. R. Briggs
Lawrence Livermore National Lab.
Attn: (L-71)
P.O. Box 808
Livermore, CA 94550

Dr. D. L. Bullock
Optical Sciences Department
TRW Space and Technology Group
Redondo Beach, CA 90278

Dr. Fred Burskirk
Physics Department
Naval Postgraduate School
Monterey, CA 93940

Dr. Ken Busby
Mission Research Corporation
1720 Randolph Road, S.E.
Albuquerque, NM 87106

Dr. K. J. Button
Francis Bitter Natl. Magnet Lab.
M. I. T. Branch, Box 72
Cambridge, MA 02139-0901

Dr. J. A. Byers
Lawrence Livermore National Lab.
Attn: (L-630)
P. O. Box 808
Livermore, CA 94550

Dr. Gregory Canavan
Office of Inertial Fusion
U.S. Dept. of Energy
M.S. C404
Washington, DC 20545

Dr. Malcolm Caplan
4219 Garland Drive
Fremont, CA 94536

Dr. Maria Caponi
TRW, Building R-1, Room 1184
One Space Park
Redondo Beach, CA 90278

Dr. B. Carlsten
Los Alamos National Laboratory
P. O. Box 1663
Los Alamos, NM 87545

Dr. A. Carmichael
U. S. Army - FTC
P. O. Box 1500
Huntsville, AL 35807-3801

Dr. J. Cary
University of Colorado
Box 391
Boulder, CO 80309

Prof. William Case
Dept. of Physics
Grinnell College
Grinnell, IA 50112

Dr. R. Center
Math. Sci. NW., Inc.
2755 Northup Way
Bellevue, WA 98004

Prof. Frank Chan
School of Eng. & Applied Sciences
Univ. of Calif. at Los Angeles
7731 K Boelter Hall
Los Angeles, CA 90024

Dr. K. C. Chan
Los Alamos National Laboratory
P. O. Box 1663
Los Alamos, NM 87545

Dr. V. S. Chan
GA Technologies
P.O. Box 85608
San Diego, CA 92138

Dr. Will E. Chandler
Pacific Missile Test Center
Code 0141-5
Point Muga, CA 93042

Dr. J. Chase
Lawrence Livermore National Laboratory
P. O. Box 808
Livermore, CA 94550

Dr. S. Chattopadhyay
Lawrence Berkeley Laboratory
University of California, Berkeley
Berkeley, CA 94720

Dr. S. Chen
MIT Plasma Fusion Center
NW16-176
Cambridge, MA 01890

Dr. Yu-Juan Chen
L-626
Lawrence Livermore National Laboratory
P. O. Box 808
Livermore, CA 94550

Dr. D. P. Chernin
Science Applications Intl. Corp.
1720 Goodridge Drive
McLean, VA 22102

Dr. Art Chester
Hughes E51
Mail Stop A269
P.O. Box 902
El Segundo, CA 90245

Dr. Abraham Chian
IGPD
Univ. of Calif. at Los Angeles
Los Angeles, CA 90024

Dr. S. C. Chiu
GA Technologies Inc.
P.O. Box 85608
San Diego, CA 92138

Dr. Y. C. Cho
NASA-Lewis Research Center
Mail Stop-54-5
Cleveland, Ohio 44135

Dr. J. Christiansen
Hughes Aircraft Co.
Electron Dynamics Division
3100 West Lomita Blvd.
Torrance, CA 90509

Dr. T. L. Churchill
Spectra Technology, Inc.
2755 Northup Way
Bellevue, WA 98004

Major Bart Clare
USASDC
P. O. BOX 15280
Arlington, VA 22215-0500

Dr. Melville Clark
8 Richard Road
Wayland, MA 01778

Dr. Robert Clark
P.O. Box 1925
Washington, D.C. 20013

Dr. David B. Cline
The Inst. for Accelerator Physics
Department of Physics
University of Wisconsin-Madison
Madison, WI 53706

Dr. Alan J. Cole
TRW
One Space Park
Redondo Beach, CA 90278

Dr. William Colson
Berkeley Research Asso.
P. O. Box 241
Berkeley, CA 94701

Dr. William Condell
Office of Naval Research
Attn: Code 421
800 N. Quincy St.
Arlington, VA 22217

Dr. Richard Cooper
Los Alamos National Scientific
Laboratory
P.O. Box 1663
Los Alamos, NM 87545

Dr. Robert S. Cooper
Director, DARPA
1400 Wilson Boulevard
Arlington, VA 22209

Dr. M. Cornacchia
Lawrence Berkeley Laboratory
University of California, Berkeley
Berkeley, CA 94720

Dr. R. A. Cover
Rockwell International/Rocketdyne Div.
6633 Canoga Avenue, FA-38
Canoga Park, CA 91304

Dr. D. Crandall
ER-55, GTN
Department of Energy
Washington, DC 20545

Dr. M. S. Curtin
KMS Fusion, Inc.
P.O. Box 1567
Ann Arbor, MI 48106

Dr. Antonello Cutolo
Research Associate
Hansen Labs
NEPL Annex
Stanford University
Stanford, CA 94305

Dr. Bruce Danly
MIT
NW16-174
Cambridge, MA 02139

Dr. R. Davidson (5 copies)
Plasma Fusion Center
Mass. Institute of Tech.
Cambridge, MA 02139

Dr. John Dawson (4 copies)
Physics Department
University of California
Los Angeles, CA 90024

Dr. David A. G. Deacon
Deacon Research
Suite 203
900 Welch Road
Palo Alto, CA 94306

Dr. T. L. Deloney
Dept. of Electrical Engineering
Stanford University
Stanford, CA 94305

Deputy Under Secretary of
Defense for R&AT
Room 3E114, The Pentagon
Washington, D.C. 20301

Prof. P. Diament
Dept. of Electrical Engineering
Columbia University
New York, NY 10027

Dr. N. Dionne
Raytheon Company
Microwave Power Tube Division
Foundry Avenue
Waltham, MA 02154

Director
National Security Agency
Fort Meade, MD 20755
ATTN: Dr. Richard Foss, A42
Dr. Thomas Handel, A243
Dr. Robert Madden, R/SA

Director of Research (2 copies)
U. S. Naval Academy
Annapolis, MD 21402

Dr. T. Doering
Boeing Aerospace Company
P.O. Box 3999
Seattle, WA 98124

Dr. Gunter Dohler
Northrop Corporation
Defense Systems Division
600 Hicks Road
Rolling Meadows, IL 60008

Dr. Franklin Dolezal
Hughes Research Laboratory
3011 Malibu Canyon Rd.
Malibu, CA 90265

Dr. A. Drobot
Science Applications Intl. Corp.
1710 Goodridge Road
McLean, VA 22102

Dr. Dwight Duston
Strategic Defense Initiative Org.
OSD/SDIO/IST
Washington, DC 20301-7100

Dr. Joseph Eberly
Physics Department
Univ. of Rochester
Rochester, NY 14627

Dr. J. A. Edighoffer
TRW, Bldg. R-1
One Space Park
Redondo Beach, CA 90278

Dr. O. C. Eldridge
University of Wisconsin
1500 Johnson Drive
Madison, WI 53706

Dr. Luis R. Elias (2 copies)
Quantum Institute
University of California
Santa Barbara, CA 93106

Dr. C. J. Elliott
Los Alamos National Laboratory
P. O. Box 1663
Los Alamos, NM 87545

Dr. James Elliott
X1-Division, M.S. 531
Los Alamos Natl. Scientific Lab.
P. O. Box 1663
Los Alamos, NM 87545

Dr. A. England
Oak Ridge National Laboratory
P.O. Box Y
Mail Stop 3
Building 9201-2
Oak Ridge, TN 37830

Dr. William M. Fairbank
Phys. Dept. & High Energy
Phys. Laboratory
Stanford University
Stanford, CA 94305

Dr. Anne-Marie Fauchet
Brookhaven National Laboratories
Associated Universities, Inc.
Upton, L.I., NY 11973

Dr. J. Feinstein
Dept. of Electrical Engineering
Stanford University
Stanford, CA 94305

Dr. Frank S. Felber
11011 Torreyana Road
San Diego, CA 92121

Dr. D. Feldman
Los Alamos National Laboratory
P. O. Box 1663
Los Alamos, NM 87545

Dr. Renee B. Feldman
Los Alamos National Laboratory
P. O. Box 1663
Los Alamos, NM 87545

Dr. L. A. Ferrari
Queens College
Department of Physics
Flushing, NY 11367

Dr. C. Finfgeld
ER-542, GTN
Department of Energy
Washington, DC 20545

Dr. A. S. Fisher
Dept. of Electrical Engineering
Stanford University
Stanford, CA 94305

Dr. R. G. Fleig
Hughes Research Laboratory
3011 Malibu Canyon Road
Malibu, CA 90265

Dr. H Fleischmann
Cornell University
Ithaca, NY 14850

Dr. E. Fontana
Dept. of Electrical Engineering
Stanford University
Stanford, CA 94305

Dr. Norval Fortson
University of Washington
Department of Physics
Seattle, WA 98195

Dr. Roger A. Freedman
Quantum Institute
University of California
Santa Barbara, CA 93106

Dr. Lazar Friedland
Dept. of Eng. & Appl. Science
Yale University
New Haven, CT 06520

Dr. Walter Friez
Air Force Avionics Laboratory
AFWAL/AADM-1
Wright/Paterson AFB, OH 45433

Dr. Shing F. Fung
Code 696
GSFC
NASA
Greenbelt, MD 20771

Dr. R. Gajewski
Div. of Advanced Energy Projects
U. S. Dept of Energy
Washington, DC 20545

Dr. H. E. Gallagher
Hughes Research Laboratory
3011 Malibu Canyon Road
Malibu, CA 90265

Dr. James J. Gallagher
Georgia Tech. EES-EOD
Baker Building
Atlanta, GA 30332

Dr. W. J. Gallagher
Boeing Aerospace Co.
P. O. Box 3999
Seattle, WA 98124

Dr. J. Gallardo
Quantum Institute
University of California
Santa Barbara, CA 93106

Dr. E. P. Garate
Dept. of Physics and Astronomy
Dartmouth College
Hanover, NH 03755

Dr. A. Garren
Lawrence Berkeley Laboratory
University of California, Berkeley
Berkeley, CA 94720

Dr. Richard L. Garwin
IBM, T. J. Watson Research Ctr.
P.O. Box 218
Yorktown Heights, NY 10598

Dr. J. Gea-Banacloche
Dept. of Physics & Astronomy
Univ. of New Mexico
800 Yale Blvd. NE
Albuquerque, NM 87131

DR. R. I. Gellert
Spectra Technology
2755 Northup Way
Bellevue, WA 98004

Dr. T. V. George
EP-531, GTN
Department of Energy
Washington, DC 20545

Dr. Edward T. Gerry, President
W. J. Schafer Associates, Inc.
[illegible] N. [illegible] Myer Drive
Arlington, VA 22209

Dr. Roy Glauber
Physics Department
Harvard University
Cambridge, MA 02138

Dr. B. B. Godfrey
Mission Research Corporation
1720 Randolph Road, S. E.
Albuquerque, NM 87[illegible]

Dr. John C. Goldstein, X-1
Los Alamos Natl. Scientific Lab.
P.O. Box 1663
Los Alamos, NM 87545

Dr. Yee Fu Goul
Plasma Physics Lab., Rm 102
S.W. Mudd
Columbia University
New York, NY 10027

Dr. C. Grabbe
Department of Physics
University of Iowa
Iowa City, Iowa 52242

Dr. V. L. Granatstein
Dept. of Electrical Engineering
University of Maryland
College Park, MD 20742

Dr. D. D. Gregoire
Quantum Institute and Dept. of Physics
University of California
Santa Barbara, CA 93106

Dr. Y. Greenzweig
Quantum Inst. and Dept. of Physics
University of California
Santa Barbara, CA 93106

Dr. Morgan K. Grover
R&D Associates
P. O. Box 9695
4640 Admiralty Highway
Marina Del Rey, CA 90291

Dr. A. H. Guenter
Air Force Weapons Laboratory
Kirtland AFB, NM 87117

Dr. K. Das Gupta
Physics Department
Texas Tech University
Lubbock, TX 79409

Dr. Benjamin Haberman
Associate Director, OSTP
Room 476, Old Exe. Office Bldg.
Washington, D.C. 20506

Dr. R. F. Hagland, Jr.
Director, Vanderbilt University
Nashville, TN 37235

Dr. K. Halbach
Lawrence Berkeley Laboratory
University of California, Berkeley
Berkeley, CA 94720

Dr. P. Hammerling
La Jolla Institute
P.O. Box 1434
La Jolla, CA 92038

Dr. R. Harvey
Hughes Research Laboratory
3011 Malibu Canyon Road
Malibu, CA 90265

Prof. Herman A Haus
Mass. Institute of Technology
Rm. 36-351
Cambridge, MA 02139

Dr. S. Hawkins
Lawrence Livermore National Laboratory
P. O. Box 808
Livermore, CA 94550

Dr. Rod Hiddleston
KMS Fusion
3621 South State Road
P. O. Box 1567
Ann Arbor, MI 48106

Dr. J. L. Hirshfield (2 copies)
Yale University
Mason Laboratory
400 Temple Street
New Haven, CT 06520

Dr. K. Hizanidis
Physics Dept.
University of Maryland
College Park, MD 20742

Dr. A. H. Ho
Dept. of Electrical Engineering
Stanford University
Stanford, CA 94305

Dr. Darwin Ho
L-477
Lawrence Livermore National Laboratory
P. O. Box 808
Livermore, CA 94550

Dr. J. Hoffman
Sandia National Laboratories
ORG. 1231, P.O. Box 5800
Albuquerque, NM 87185

Dr. R. Hofland
Aerospace Corp.
P. O. Box 92957
Los Angeles, CA 90009

Dr. Fred Hopf
Optical Sciences Building, Room 602
University of Arizona
Tucson, AZ 85721

Dr. Heinrich Hora
Iowa Laser Facility
University of Iowa
Iowa City, Iowa

Dr. J. Y. Hsu
General Atomic
San Diego, CA 92138

Dr. H. Hsuan
Princeton Plasma Physics Lab.
James Forrestal Campus
P.O. Box 451
Princeton, NJ 08544

Dr. James Hu
Quantum Inst. and Phys. Dept.
University of California
Santa Barbara, CA 93106

Dr. Benjamin Hubberman
Associate Director, OSTP
Rm. 476, Old Executive Office Bldg.
Washington, DC 20506

Dr. J. Hyman
Hughes Research Laboratory
3011 Malibu Canyon Road
Malibu, CA 90265

Dr. H. Ishizuka
University of California
Department of Physics
Irvine, CA 92717

Dr. A. Jackson
Lawrence Berkeley Laboratory
University of California, Berkeley
Berkeley, CA 94720

Dr. S. F. Jacobs
Optical Sciences Center
University of Arizona
Tucson, AZ 85721

Dr. Pravin C. Jain
Asst. for Communications Tech.
Defense Communications Agency
Washington, DC 20305

Dr. E. T. Jaynes
Physics Department
Washington University
St. Louis, MO 63130

Dr. B. Carol Johnson
Ctr. for Radiation Research
National Bureau of Standards
Gaithersburg, MD 20899

Dr. Bernadette Johnson
Lincoln Laboratory
Lexington, MA 02173

Dr. Richard Johnson
Physics International
2700 Merced St.
San Leandro, CA 94577

Dr. G. L. Johnston
NW 16-232
Mass. Institute of Tech.
Cambridge, MA 02139

Dr. Shayne Johnston
Physics Department
Jackson State University
Jackson, MS 39217

Dr. William Jones
U. S. Army SDC
P. O. Box 1500
Huntsville, Al 35807-3801

Dr. F. A. Jong
Lawrence Livermore National Laboratory
P. O. Box 808/L626
Livermore, CA 94550

Dr. Howard Jory (3 copies)
Varian Associates, Bldg. 1
611 Hansen Way
Palo Alto, CA 94303

Dr. C. Joshi
University of California
Los Angeles, CA 90024

Dr. Paul Kennedy
Rockwell International/Rocketdyne Div.
6633 Canoga Avenue, FA-40
Canoga Park, CA 91304

Dr. R. Kennedy
Boeing Aerospace Company
P.O. Box 3999
Seattle, WA 98124

Dr. K. J. Kim, MS-101
Lawrence Berkeley Lab.
Rm. 223, B-80
Berkeley, CA 94720

Dr. I. Kimel
Quantum Institute
University of California
Santa Barbara, CA 93106

Dr. Brian Kincaid
AT&T Bell Labs
700 Mountain Ave.
Murray Hill, NJ 07974

Dr. S. P. Kno
Polytechnic Institute of NY
Route 110
Farmingdale, NY 11735

Dr. Xu Knogyi
Room 36-285
Mass. Institute of Technology
Cambridge MA 02139

Dr. A. Kolb
Maxwell Laboratories, Inc.
8835 Balboa Avenue
San Diego, CA 92123

Dr. Eugene Kopf
Principal Deputy Assistant
Secretary of the Air Force (RD&L)
Room 4E964, The Pentagon
Washington, D.C. 20330

Dr. P. Korn
Maxwell Laboratories, INc.
8835 Balboa Avenue
San Diego, CA 92123

Dr. S. Krinsky
Nat. Synchrotron Light Source
Brookhaven National Laboratory
Upton, NY 11973

Prof. N. M. Kroll
Department of Physics
B-019, UCSD
La Jolla, CA 92093

Dr. Thomas Kwan
Los Alamos National Scientific
Laboratory, MS608
P. O. Box 1663
Los Alamos, NM 87545

Dr. Jean Labacqz
Stanford University
SLAC
Stanford, CA 94305

Dr. Ross H. Labbe
Rockwell International/Rocketdyne Div.
6633 Canoga Avenue, FA-40
Canoga Park, CA 91304

Dr. Willis Lamb
Optical Sciences Center
University of Arizona
Tucson, AZ 87521

Dr. H. Lancaster
Lawrence Berkeley Laboratory
University of California, Berkeley
Berkeley, CA 94720

Dr. D. J. Larson
The Inst. for Accelerator Physics
Department of Physics
University of Wisconsin-Madison
Madison, WI 53706

Dr. J. LaSala
Physics Dept.
U. S. M. A.
West Point, NY 10996

Dr. Bernard Laskowski
M.S. 230-3
NASA-Ames
Moffett Field, CA 94305

Dr. Charles J. Lasnier
TPW
High Energy Physics Lab.
Stanford University
Stanford, CA 94305

Dr. Michael Lavan
U.S. Army Strategic Def. Command
ATTN: Code CSSD-H-D
P. O. Box 1500
Huntsville, AL 35807-3801

Dr. Ray Leadabrand
SRI International
333 Ravenswood Avenue
Menlo Park, CA 94025

Dr. Kotik K. Lee
Perkin-Elmer
Optical Group
100 Wooster Heights Road
Danbury, CT 06810

Dr. K. Lee
Los Alamos Nat. Scientific Lab.
Attn: X-1 MS-E531
P. O. Box 1663
Los Alamos, NM 87545

Dr. Barry Leven
NISC/Code 20
4301 Suitland Road
Washington, D.C. 20390

Dr. B. Levush
University of Maryland
College Park, MD 20742

Dr. Lewis Licht
Department of Physics
Box 4348
U. of Illinois at Chicago Cir.
Chicago, IL 60680

Dr. M. A. Lieberman
Dept. EECS
Univ. of Cal. at Berkeley
Berkeley, CA 94720

Dr. Anthony T. Lin
Dept. of Physics
University of California
Los Angeles, CA 90024

Dr. B. A. Lippmann
Stanford Linear Accel. Center
BIN 26
Stanford, CA 94305

Dr. R. Lohsen
Los Alamos National Laboratory
P. O. Box 1663
Los Alamos, NM 87545

Dr. D. D. Lowenthal
Spectra Technology
2755 Northup Way
Bellevue, WA 98004

Dr. A. Luccio
Brookhaven National Laboratory
Accelerator Dept.
Upton, NY 11973

Dr. A. Lumpkin
Los Alamos National Laboratory
P. O. Box 1663
Los Alamos, NM 87545

Dr. Phil Mace
W. J. Shafer Assoc.,Inc.
1901 N. Fort Myer Drive
Arlington, VA 22209

Dr. John Madey
S.P.R.C.
Physics Department
Stanford University
Stanford, CA 94305

Dr. Siva A. Mani
Science Applications Intl. Corp.
1040 Waltham Street
Lexington, MA 02173-8027

Dr. J. Mark
Lawrence Livermore National Lab.
Attn: L-477
P. O. Box 808
Livermore, CA 94550

Dr. T. C. Marshall
Applied Physics Department
Columbia University
New York, NY 10027

Dr. Xavier K. Maruyama
Dept. of Physics
Naval Postgraduate School
Monterey, CA 93943

Dr. Neville Marzwell
Jet Propulsion Lab.
MS 198-330
4800 Oak Grove Drive
Pasadena, CA 91109

Dr. A. Maschke
TRW
Mail Stop 01-1010
1 Space Park
Redondo Beach CA 90278

Dr. Joseph Mathew
Sachs/Freeman Associate
Landover, MD 20784

Dr. K. Matsuda
GA Technologies Inc.
P.O. Box 85608
San Diego, CA 92138

Dr. John McAdoo
Mission Research Corporation
5503 Cherokee Ave., Suite 201
Alexandria, Va 22312

Dr. D. B. McDermott
Electrical Engineering Dept.
University of California
Los Angeles, CA 90024

Dr. J. K. McIver
Dept. of Physics & Astronomy
Univ. of New Mexico
800 Yale Blvd. NE
Albuquerque, NM 87131

Dr. C. McKinstrie
MS B258
P.O. Box 1663
Los Alamos, NM 87545

Col J. F. McNulty
Ground Based Laser Proj. Office
DASD-H-F
White Sands Missile Range, NM 88002-1198

Dr. B. McVey
Los Alamos National Laboratory
P. O. Box 1663
Los Alamos, NM 87545

Dr. John Meson
DARPA
1400 Wilson Boulevard
Arlington, VA 22209

Col Thomas Meyer
DARPA/STO
1400 Wilson Boulevard
Arlington, VA 22209

Dr. F. E. Mills
Fermilab
P.O., Box 500
Batavia, IL 60510

Dr. D. R. Mize
Hughes Research Laboratory
3011 Malibu Canyon Road
Malibu, CA 90265

Dr. Mel Month
Brookhaven National Laboratories
Associated Universities, Inc.
Upton, L.I., NY 11973

Dr. B. N. Moore
Austin Research Assoc.
1901 Rutland Dr.
Austin, TX 78758

Dr. Gerald T. Moore
University of New Mexico
Albuquerque, NM 87131

Dr. Warren Mori
1-130 Knudsen Hall
U.C.L.A.
Los Angeles, CA 90024

Dr. Philip Morton
Stanford Linear Accelerator Center
P.O. Box 4349
Stanford, CA 94305

Dr. Jesper Munch
TRW
One Space Park
Redondo Beach, CA 90278

Dr. James S. Murphy
National Synchrotron Light Source
Brookhaven National Laboratory
Upton, NY 11975

Dr. J. Nation
Cornell University
Ithaca, NY 14850

Dr. R. Neighbours
Physics Department
Naval Postgraduate School
Monterey, CA 93943

Dr. George Neil
TRW
One Space Park
Redondo Beach, CA 90278

Dr. Kelvin Neil
Lawrence Livermore National Lab.
Code L-321, P.O. Box 808
Livermore, CA 94550

Dr. W. M. Nevins
L-639
Lawrence Livermore National Laboratory
P. O. Box 808
Livermore, CA 94550

Dr. Brian Newnam
MSJ 564
Los Alamos National Scientific Lab.
P.O. Box 1663
Los Alamos, NM 87545

Dr. W. Nexsen
Lawrence Livermore National Laboratory
P. O. Box 808
Livermore, CA 94550

Lt. Rich Nielson/ESD/INK
Hanscomb Air Force Base
Stop 21, MA 01731

Dr. Milton L. Noble (2 copies)
General Electric Company
G. E. Electric Park
Syracuse, NY 13201

Dr. K. O'Brien
Div. 1241 SNLA
Albuquerque, NM 87185

Dr. John D. O'Keefe
TRW
One Space Park
Redondo Beach, CA 90278

Dr. T. Orzechowski
L-436
Lawrence Livermore National Lab.
P. O. Box 808
Livermore, CA 94550

Prof. E. Ott (2 copies)
Department of Physics
University of Maryland
College Park, MD 20742

OUSDRE (R&AT)
Room 3D1067, The Pentagon
Washington, D.C. 20301

Dr. A. J. Palmer
Hughes Research Laboratory
3011 Malibu Canyon Road
Malibu, CA 90265

Dr. Robert B. Palmer
Brookhaven National Laboratories
Associated Universities, Inc.
Upton, L.I., NY 11973

Dr. J. Palmer
Hughes Research Laboratory
Malibu, CA 90265

Dr. Richard H. Pantell
Stanford University
Stanford, CA 94305

Dr. Dennis Papadopoulos
Astronomy Department
University of Maryland
College Park, Md. 20742

Dr. P. Parks
GA Technologies
P.O. Box 85608
San Diego, Ca 92138

Dr. John A. Pasour
Mission Research Laboratory
5503 Cherokee Avenue
Alexandria, VA

Dr. C. K. N. Patel
Bell Laboratories
Murray Hill, NJ 07974

Dr. Richard M. Patrick
AVCO Everett Research Lab., Inc.
2385 Revere Beach Parkway
Everett, MA 02149

Dr. Claudio Pellegrini
Brookhaven National Laboratory
Associated Universities, Inc.
Upton, L.I., NY 11973

Dr. Samuel Penner
Center for Radiation Research
National Bureau of Standards
Gaithersburg, MD 20899

Dr. D. E. Pershing
Mission Research Corporation
5503 Cherokee Avenue
Alexandria, VA 22312

Dr. J. M. Peterson
Lawrence Berkeley Laboratory
University of California, Berkeley
Berkeley, CA 94720

Dr. M. Piestrup
Adelphi Technology
13800 Skyline Blvd. No. 2
Woodside, CA 94062 CA 94305

Dr. Alan Pike
DARPA
1400 Wilson Boulevard
Arlington, VA 22209

Dr. Hersch Pilloff
Code 421
Office of Naval Research
Arlington, VA 22217

Dr. A. L. Pindroh
Spectra Technology
2755 Northup Way
Bellevue, WA 98004

Dr. D. J. Pistoresi
Boeing Aerospace Company
P. O. Box 3999
Seattle, WA 98124-2499

Dr. Peter Politzer
General Atomic Tech., Rm. 13/260
P. O. Box 85608
San Diego, CA 92138

Major Donald Ponikvar
U. S. Army SDC
P. O. Box 15280
Arlington, VA 22245-0280

Dr. S. E. Poor
Lawrence Livermore National Laboratory
P. O. Box 808
Livermore, CA 94550

Prof. M. Porkolab
NW 36-213
Mass. Institute of Technology
Cambridge, MA 02139

Dr. R. V. Pound
Physics Department
Harvard University
Cambridge, MA 02138

Mr. J. E. Powell
Sandia National Laboratories
ORG. 1231, P.O. Box 5800
Albuquerque, NM 87185

Dr. Mark A. Prelas
Nuclear Engineering
Univ. of Missouri-Columbia
1033 Engineering
Columbia, Missouri 65211

Dr. Donald Prosnitz
Lawrence Livermore National Lab.
Attn: L-470
P. O. Box 808
Livermore, CA 94550

Dr. D. C. Quimby
Spectra Technology
2755 Northup Way
Bellevue, WA 98004

Dr. Paul Rabinowitz
Xexon Research and Eng. Comp.
P. O. Box 45
Linden, NJ 07036

Dr. G. Ramian
Quantum Institute
University of California
Santa Barbara, CA 93106

Dr. L. Ranjun
Dept. of Physics
University of Cal. at Irvine
Irvine, CA 92717

Dr. L. L. Reginato
Lawrence Livermore National Laboratory
P. O. Box 808
Livermore, CA 94550

Dr. M. B. Reid
Dept. of Electrical Engineering
Stanford University
Stanford, CA 94305

Dr. D. A. Reilly
AVCO Everett Research Lab.
Everett, MA 02149

Dr. M. Reiser
University of Maryland
Department of Physics
College Park, MD 20742

Dr. Bruce A. Richman
High Energy Physics Lab.
Stanford University
Stanford, CA 94305

Dr. S. Ride
Johnson Space Center
Houston, TX 77058

Dr. C. W. Roberson
Code 412
Office of Naval Research
800 N. Quincy Street
Arlington, VA 22217

Dr. B. Robinson
Boeing Aerospace Company
P.O. Box 3999
Seattle, WA 98124

Dr. K. Robinson
Spectra Technology
2755 Northup Way
Bellevue, WA 98004

Dr. D. Rogers
Lawrence Livermore National Laboratory
P. O. Box 808
Livermore, CA 94550

Dr. Jake Romero
Boeing Aerospace Company
P. O. Box 3999
Seattle, WA 98124-2499

Dr. T. Romesser
TRW, Inc.
One Space Park
Redondo Beach, Ca 90278

Dr. Marshall N. Rosenbluth
Institute for Fusion Studies
The Univ. of Texas at Austin
Austin, TX 78712

Dr. J. B. Rosenzweig
The Inst. for Accelerator Physics
Department of Physics
University of Wisconsin-Madison
Madison, WI 53706

Dr. J. Ross
Spectra Technology
2755 Northup Way
Bellevue, WA 98004

Dr. N. Rostoker
University of California
Department of Physics
Irvine, CA 92717

Dr. G. A. Saenz
Hughes Research Laboratory
3011 Malibu Canyon Road
Malibu, CA 90265

Dr. Antonio Sanchez
Lincoln Laboratory
Mass. Institute of Tech.
Room B213
P. O. Box 73
Lexington, MA 02173

Dr. Aldric Saucier
BMD-PO
Ballistic Missile Defense
Program Office
P. O. Box 15280
Arlington, VA 22215

Dr. A. Saxman
Los Alamos National Scientific Lab.
P. O. Box 1663, MSE523
Los Alamos, NM 87545

Dr. J. Scharer
ECE Dept.
Univ. of Wisconsin
Madison, WI 53706

Dr. E. T. Scharlemann
L626
Lawrence Livermore National Laboratory
P. O. Box 808
Livermore, CA 94550

Prof. S. P. Schlesinger
Dept. of Electrical Engineering
Columbia University
New York, NY 10027

Dr. Howard Schlossberg
AFOSR
Bolling AFB
Washington, D.C. 20332

Dr. George Schmidt
Stevens Institute of Technology
Physics Department
Hoboken, NJ 07030

Dr. M. J. Schmitt
Los Alamos National Laboratory
P. O. Box 1663
Los Alamos, NM 87545

Dr. Stanley Schneider
Rotodyne Corporation
26628 Fond Du Lac Road
Palos Verdes Peninsula, CA 90274

Dr. N. Schoen
TRW DSSG
One Space Park
Redondo Beach, CA 90278

Dr. M. L. Scott
Los Alamos National Laboratory
P. O. Box 1663
Los Alamos, NM 87545

Dr. Richard L. Schriever (DP-23)
Director, Office of Inertial Fusion
U. S. Department of Energy
Washington, D.C. 20545

Dr. R. W. Schumacher
Hughes Research Laboratories
3011 Malibu Canyon Road
Malibu, CA 09265

Dr. H. Schwettmann
Phys. Dept. & High Energy
Physics Laboratory
Stanford University
Stanford, CA 94305

Dr. Marlan O. Scully
Dept. of Physics & Astronomy
Univ. of New Mexico
800 Yale Blvd. NE
Albuquerque, NM 87131

Dr. S. B. Segall
KMS Fusion
3941 Research Park Dr.
P.O. Box 1567
Ann Arbor, MI 48106

Dr. Robert Sepucha
DARPA
1400 Wilson Boulevard
Arlington, VA 22209

Prof. P. Serafim
Northeastern University
Boston, MA 02115

Dr. A. M. Sessler
Lawrence Berkeley Laboratroy
University of California
1 Cyclotron Road
Berkeley, CA 94720

Dr. W. Sharp
L-626
Lawrence Livermore National Laboratory
P. O. Box 808
Livermore, CA 94550

Dr. Earl D. Shaw
Bell Laboratories
600 Mountain Avenue
Murray Hill, NJ 07974

Dr. J. P. Sheerim
KMS Fusion
P.O. Box 1567
Ann Arbor, MI 48106

Dr. R. Shefer
Science Research Laboratory
15 Ward Street
Somerville, MA 02143

Dr. R. L. Sheffield
Los Alamos National Laboratory
P.O. Box 1663
Los Alamos, NM 87545

Dr. Shemwall
Spectra Technology
2755 Northup Way
Bellevue, WA 98004

Dr. Shen Shey
DARPA/DEO
1400 Wilson Boulevard
Arlington, VA 22209

Dr. D. Shoffstall
Boeing Aerospace Company
P.O. Box 3999
Seattle, WA 98124

Dr. I. Shokair
SNLA, Org. 1271
Albuquerque, NM 87185

Dr. J. S. Silverstein
Harry Diamond Laboratories
2800 Powder Mill Road.
Adelphi, MD 20783

Dr. Jack Slater
Spectra Technology
2755 Northup Way
Bellevue, WA 98004

Dr. Kenneth Smith
Physical Dynamics, Inc.
P.O. Box 556
La Jolla, CA 92038

Dr. Lloyd Smith
Lawrence Berkeley Laboratory
University of California
1 Cyclotron Road
Berkeley, CA 94720

Dr. Stephen J. Smith
JILA
Boulder, CO 80302

Dr. T. Smith
TRW, Inc.
One Apace Park
Redondo Beach, CA 90278 R1/2044

Dr. Todd Smith
Hansen Labs
Stanford University
Stanford, CA 94305

Dr. Joel A. Snow, M.S. E084
Senior Technical Advisor
Office of Energy Research
U. S. Department of Energy
Washington, D.C. 20585

Dr. J. Z. Soln (22300)
Harry Diamond Laboratories
2800 Powder Mill Road
Adelphi, MD 20783

Dr. G. Spalek
Los Alamos National Laboratory
P. O. Box 1663
Los Alamos, NM 87545

Dr. Richard Spitzer
Stanford Linear Accelerator Center
P.O. Box 4347
Stanford, CA 94305

Mrs. Alma Spring
DARPA/Administration
1400 Wilson Boulevard
Arlington, VA 22209

SRI/MP Reports Area G037 (2 copies)
ATTN: D. Leitner
333 Ravenswood Avenue
Menlo Park, CA 94025

Dr. W. Stein
Los Alamos National Laboratory
P. O. Box 1663
Los Alamos, NM 87545

Dr. L. Steinhauer
STI
2755 Northup Way
Bellevue, WA 98004

Dr. Efrem J. Sternbach
Lawrence Berkeley Laboratory
University of California, Berkeley
Berkeley, CA 94720

Dr. M. Strauss
Department of Physics
University of California at Irvine
Irvine, CA 92717

Dr. W. C. Stwalley
Iowa Laser Facility
University of Iowa
Iowa City, Iowa

Dr. R. Sudan
Lab. of Plasma Studies
Cornell University
Ithaca, NY 14850

Dr. P. W. Sumner
Hughes Research Laboratory
3011 Malibu Canyon Road
Malibu, CA 90265

Dr. David F. Sutter
ER 224, GTN
Department of Energy
Washington, D.C. 20545

Dr. Abraham Szoke
ML/L-470
Lawrence Livermore Natl. Lab.
P.O. Box 808
Livermore, CA 94550

Dr. R. Taber
Dept. of Phys. & High Energy Lab.
Stanford University
Stanford, CA 94305

Dr. T. Tajima
IFS
Univ. of Texas
Austin, TX 78712

Dr. H. Takeda
Los Alamos National Laboratory
P. O. Box 1663
Los Alamos, NM 87545

Dr. J. J. Tancredi
Hughes Aircraft Co.
Electron Dynamics Division
3100 West Lomita Blvd.
Torrance, CA 90509

Dr. Milan Tekula
AVCO Everett Research Lab.
2385 Revere Beach Parkway
Everett, MA 02149

Dr. R. Temkin (2 copies)
Mass. Institute of Technology
Plasma Fusion Center
Cambridge, MA 02139

Dr. L. Thode
Los Alamos National Laboratory
P. O. Box 1663
Los Alamos, NM 87545

Dr. Keith Thomassen, L-637
Lawrence Livermore National Laboratory
P. O. Box 808
Livermore, CA 94550

Dr. Harold Thompson
TRW, Inc.
R1/2120
One Space Park
Redondo Beach, Ca 90278

Dr. Norman H. Tolk
Physics Department
Vanderbilt University
Nashville, TN 37240

Dr. Kang Tsang
Science Applications Intl. Corp.
10260 Campus Point Drive
San Diego, CA 92121

Dr. E. Tyson
Boeing Aerospace Company
P.O. Box 3999
Seattle, WA 98124

Dr. H. S. Uhm
Naval Surface Warfare Center
White Oak Lab.
Silver Spring, MD 20903-5000

Dr. L. Ulstrup
TRW, Inc.
One Space Park
Redondo Beach, Ca 90278

Under Secretary of Defense (R&E)
Office of the Secretary of Defense
Room 3E1006, The Pentagon
Washington, D.C. 20301

Dr. L. Vahala
Physics Dept.
College of William & Mary
Williamsburg, VA .23185

Dr. A. Valla
Spectra Technology
2755 Northup Way
Bellevue, WA 98004

Dr. A. Vetter
Boeing Aerospace Company
P.O. Box 3999
Seattle, WA 98124

Dr. A. A. Vetter
Spectra Technology
2755 Northup Way
Bellevue, WA 98004

Dr. G. Vignola
Brookhaven National Laboratories
Associated Universities, Inc.
Upton, L.I., NY 11973

Dr. S. A. Von Laven
KMS Fusion Inc.
Ann Arbor, MI 48106

Dr. John E. Walsh
Wilder Laboratory
Department of Physics (HB 6127)
Dartmouth College
Hanover NH 03755

Dr. W. M. Walsh, Jr.
Bell Laboratories
600 Mountain Avenue
Room 1-D 332
Murray Hill, NJ 07974

Dr. Jiunn-Ming Wang
Brookhaven National Laboratories
Associated Universities, Inc.
Upton, L.I., NY 11973

Dr. T-S. Wang
Los Alamos National Laboratory
P. O. Box 1663
Los Alamos, NM 87545

Dr. J. F. Ward
University of Michigan
Ann Arbor, MI 48109

Dr. E. Warden
Code PDE 106-3113
Naval Electronics Systems Command
Washington, DC 20363

Dr. Roger W. Warren
Los Alamos National Sciencific Lab.
P.O. Box 1663
Los Alamos, NM 87545

Dr. J. Watson
Los Alamos National Laboratory
P. O. Box 1663
Los Alamos, NM 87545

Dr. B. Weber
Harry Diamond Laboratories
2800 Powder Mill Road
Adelphi, MD 20783

END
DATE
9-88
DTIC